

# EXACT CERTIFICATION OF NEURAL NETWORKS AND PARTITION AGGREGATION ENSEMBLES AGAINST LABEL POISONING

006 **Anonymous authors**

007 Paper under double-blind review

## ABSTRACT

013 Label-flipping attacks, which corrupt training labels to induce misclassifications  
 014 at inference, remain a major threat to supervised learning models. This drives the  
 015 need for robustness certificates that provide formal guarantees about a model’s  
 016 robustness under adversarially corrupted labels. Existing certification frameworks  
 017 rely on ensemble techniques such as smoothing or partition-aggregation, but treat  
 018 the corresponding base classifiers as black boxes—yielding overly conservative  
 019 guarantees. We introduce **EnsembleCert**, the first certification framework for  
 020 partition-aggregation ensembles that utilizes white-box knowledge of the base  
 021 classifiers. Concretely, EnsembleCert yields tighter guarantees than black-box ap-  
 022 proaches by aggregating per-partition white-box certificates to compute ensemble-  
 023 level guarantees in *polynomial* time. To extract white-box knowledge from the  
 024 base classifiers efficiently, we develop **ScaLabelCert**, a method that leverages the  
 025 equivalence between sufficiently wide neural networks and kernel methods using  
 026 the neural tangent kernel. ScaLabelCert yields the *first exact, polynomial-time*  
 027 calculable certificate for neural networks against label-flipping attacks. Ensemble-  
 028 Cert is either on par, or significantly outperforms the existing partition-based black  
 029 box certificates. Exemplary, on CIFAR-10, our method can certify upto **+26.5%**  
 030 more label flips in median over the test set compared to the existing black-box  
 031 approach while requiring **100** $\times$  fewer partitions, thus, challenging the prevailing  
 032 notion that heavy partitioning is a necessity for strong certified robustness.

## 1 INTRODUCTION

035 Machine learning models, especially those trained in supervised settings, are critically dependent on  
 036 the integrity of labeled data. This reliance exposes them to *label-flipping attacks*, where the training  
 037 labels are corrupted to degrade model performance, or induce targeted misclassifications (Biggio  
 038 et al., 2011; Xiao et al., 2015). In response, a range of empirical defenses have been proposed,  
 039 including data sanitization techniques that aim to identify and remove poisoned samples prior to  
 040 training (Paudice et al., 2018), and adversarial training methods that improve robustness by learning  
 041 on perturbed examples (Bal et al., 2025). However, these approaches often rely on heuristics and  
 042 have been shown to fail under adaptive attacks (Carlini & Wagner, 2017; Athalye et al., 2018; Koh  
 043 et al., 2021). This limitation has led to growing interest in *robustness certificates*, that provide formal  
 044 guarantees about the robustness of a model’s predictions under a given adversarial threat model.

045 Existing certificates against label-flipping poisoning attacks are predominantly derived using *en-*  
 046 *semble* methods. Techniques include randomized smoothing (Rosenfeld et al., 2020), where base  
 047 classifiers are trained on datasets with randomly perturbed labels, and partition aggregation (Levine  
 048 & Feizi, 2020), which trains base classifiers on *disjoint* partitions of the training data. Since these  
 049 certificates rely solely on the base classifier outputs, they are inherently black-box (Ashtiani et al.,  
 050 2020). Black-box treatment of the base classifiers often leads to overly conservative guarantees  
 051 and provides limited knowledge about the full extent of the ensemble’s robustness. One way to  
 052 understand the true robustness of the certified model is to utilize *white-box* information of the base  
 053 classifiers, i.e., white-box certificates, that leverage internal model information to yield tighter and  
 054 more informative guarantees. This raises the question: *How can we leverage white-box knowledge  
 055 of the base classifiers to derive a stronger certificate for the ensemble?*

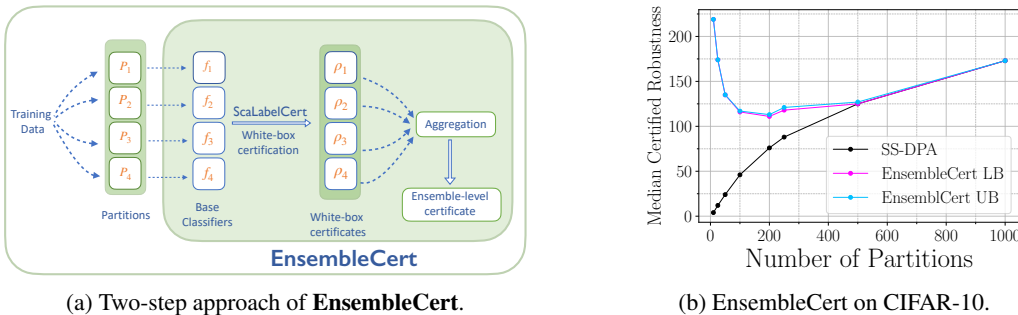


Figure 1: (a) Two-step approach of **EnsembleCert** to derive white-box guarantees for partition aggregation ensembles. (b) Evaluation on CIFAR-10 using wide neural networks trained on a regression loss as base classifiers. Using as few as 10 partitions with white-box knowledge enables the ensemble to withstand up to **26.5%** more label flips in median compared to using **1000** partitions. For a definition of the metric *median certified robustness* we refer the reader to Sec. 4.

In this work, we answer this question by proposing **EnsembleCert**, a white-box certification framework for *partition-based aggregation* ensembling techniques (Levine & Feizi, 2020). We focus specifically on the partition-based approach since they are the current state-of-the-art certifiable defense against general data poisoning attacks (Levine & Feizi, 2020; Rezaei et al., 2023; Wang et al., 2022), including label-flipping. Additionally, neural networks can be used as base classifiers in this approach, as opposed to only linear classifiers in the randomized smoothing method (Rosenfeld et al., 2020). EnsembleCert yields tighter white-box guarantees by leveraging the model information of the base classifiers following a simple two-step approach: (i) Extract white-box certificates<sup>1</sup> from the base classifiers for each partition; (ii) Aggregate the white-box certificates to derive an ensemble-wide certificate (see Fig. 1a). The problem of aggregating the partition-wise guarantees to obtain the certificate for the ensemble is formulated as an Integer Program (IP), which we show can be solved efficiently in *polynomial* time.

Thus, given a base model and a certification method for extracting white-box knowledge from the chosen base model, EnsembleCert aggregates the white-box knowledge of base classifiers to achieve ensemble-wide guarantees. In this work, we focus on deriving ensemble-level guarantees when neural networks are chosen as the base model. For certifying neural networks as base models in EnsembleCert, existing white-box approaches face significant challenges as they either rely on computationally intense Mixed Integer Linear Program (MILP) formulation (Sabanayagam et al., 2025) or loose gradient-based parameter bounding approaches (Sosnin et al., 2024). To elaborate, solving the MILP is NP-hard in the worst case, hence LabelCert (Sabanayagam et al., 2025) is practical only for datasets with a few hundred training points and does not even scale to moderately sized datasets like MNIST and CIFAR-10. On the other hand, the parameter-bounding technique (Sosnin et al., 2024) provides overly loose guarantees, leading to vacuous bounds in just few training iterations, especially for multi-class classification tasks. Furthermore, the latter method has so far been evaluated only on small multi-layer perceptrons. These limitations make the existing methods unsuitable for white-box injection into EnsembleCert, naturally raising a broader question: *Can we derive effective and scalable white-box certificates for neural networks against label-flipping attacks?*

We answer this question by developing **ScaLabelCert**, a framework that builds on the *exact* white-box method of LabelCert (Sabanayagam et al., 2025). LabelCert derives the first exact certificate for neural networks against data poisoning by leveraging the equivalence between infinitely wide Neural Networks (NNs) trained with a soft-margin loss and Support Vector Machines (SVM) using the Neural Tangent Kernel (NTK) of the network as their kernel (Chen et al., 2022; Sabanayagam et al., 2023). ScaLabelCert shows that under certain conditions, the computation complexity of LabelCert can be reduced from NP-hard to polynomial time, thus, significantly improving the scalability. Beyond the SVM formulation, ScaLabelCert further extends LabelCert by leveraging the equivalence between infinitely-wide NNs trained with a regression loss and kernel regression under the NTK (Jacot et al., 2018; Arora et al., 2019). With its ability to efficiently compute tight certificates, we adopt ScaLabelCert as our primary mechanism for injecting white-box knowledge into EnsembleCert. The tightness of the resulting partition-wise guarantees reveals the full potential of EnsembleCert and enables a reliable analysis of how partitioning contributes to robustness. Since ScaLabelCert is

---

<sup>1</sup>The specifics of white box information extracted from each base classifier are provided in Sec. 3.1

108 best suited for certifying infinite-width neural networks (see Sec. 5), we use this instantiation for our  
 109 primary evaluation. To demonstrate the applicability of EnsembleCert with finite-width networks as  
 110 base classifiers, we employ the gradient-based parameter bounding approach of (Sosnin et al., 2024)  
 111 for base-classifier certification. We detail the process of integrating the gradient-based certificate  
 112 into EnsembleCert and present the evaluation in App. C.4. Finally, to highlight that EnsembleCert is  
 113 not restricted to neural networks, we also instantiate it with a smoothed linear classifier as the base  
 114 model and apply randomized smoothing certificates (Rosenfeld et al., 2020) to each base classifier.  
 115

**Our contributions** are summarized as follows:

- 116 1. We present **EnsembleCert** in Sec. 3.1, the *first* white-box certification framework for partition  
 117 aggregation ensembles that leverages the knowledge about base-classifiers to provide white-box in-  
 118 formed certificates for the ensemble in **polynomial** time. In our experimental set-up, we evaluate  
 119 EnsembleCert with the following choices of base classifiers and corresponding certification meth-  
 120 ods: (i) Infinite-width neural networks with ScaLabelCert, (ii) Finite-width neural networks with  
 121 gradient-based parameter bounding certificate by Sosnin et al. (2024) and (iii) Smoothed linear  
 122 classifier with randomized smoothing based certificate by Rosenfeld et al. (2020).
- 123 2. With **ScaLabelCert** in Sec. 3.2, we derive the *first polynomial-time solvable exact certificate* for  
 124 infinite-width neural networks against label-flipping attacks and thus, it is the first exact certificate  
 125 for neural networks against a poisoning threat model that scales to common image benchmarks.
- 126 3. We show in Sec. 4 that for partition aggregation ensembles with a small number of partitions,  
 127 the infusion of white-box knowledge results in significant improvement in certified robustness. On  
 128 analyzing the dependence of certified robustness on the number of partitions, we demonstrate that in  
 129 certain cases, using as low as 10 partitions with white-box knowledge results in stronger robustness  
 130 guarantees in comparison to as high as 1000 partitions (see Fig. 1b). These findings call into question  
 131 the emphasis on using very large numbers of partitions to achieve good certified robustness (Levine  
 132 & Feizi, 2020), suggesting that excessively deep partitioning, which requires training a prohibitively  
 133 large number of neural networks, is not a necessity to yield strong guarantees.

## 135 2 PRELIMINARIES

137 **Notation.** Matrices are denoted by bold uppercase letters,  $\mathbf{M}$ , and vectors by bold lowercase letters,  
 138  $\mathbf{v}$ . The  $(i, j)$ -th entry of a matrix  $\mathbf{M}$  is denoted  $m_i^j$ . For a positive integer  $C$ , we write  $[C] =$   
 139  $\{1, \dots, C\}$ . The  $\ell_0$  norm is denoted by  $\|\cdot\|_0$ , and  $\mathbf{1}_{\text{condition}}$  represents the indicator function of a  
 140 given condition. We use  $\mathbf{1}^n$  for a vector of all 1s of size  $n$ . The floor operator is denoted by  $\lfloor \cdot \rfloor$ .

142 **Label-flipping and Certification.** In a supervised classification task, the training data  $\mathcal{S} = (\mathbf{X}, \mathbf{y})$   
 143 consists of feature vectors aggregated in  $\mathbf{X} \in \mathbb{R}^{n \times d}$  and labels  $\mathbf{y} \in [K]^n$ , where  $K$  is the number of  
 144 classes. A learning algorithm  $\mathcal{L}_{\text{alg}}$  takes the training set  $\mathcal{S}$  and a test sample  $\mathbf{t} \in \mathcal{T}$ , where  $\mathcal{T}$  is the  
 145 test set, as input to predict the label for  $\mathbf{t}$ , i.e.,  $\mathcal{L}_{\text{alg}}(\mathcal{S}, \mathbf{t}) \in [K]$ . In a label-flipping attack, we assume  
 146 that the adversary is allowed to change at most  $r \leq n$  training labels. Formally, an adversary can  
 147 alter the clean labels  $\mathbf{y}$  to  $\tilde{\mathbf{y}} \in \mathcal{B}_r(\mathbf{y}) := \{\tilde{\mathbf{y}} \in [K]^n \mid \|\tilde{\mathbf{y}} - \mathbf{y}\|_0 \leq r\}$  and get a perturbed training  
 148 set  $\tilde{\mathcal{S}} = (\mathbf{X}, \tilde{\mathbf{y}})$ . As the certification objective, for every  $\mathbf{t} \in \mathcal{T}$ , we aim to find the maximum number  
 149 of label flips  $\tilde{r}$  in the clean training data up to which the prediction of  $\mathcal{L}_{\text{alg}}$  for  $\mathbf{t}$  does not change, i.e.

$$151 \tilde{r}(\mathbf{t}) = \max_{\tilde{\mathcal{S}}} r \quad s.t. \quad \mathcal{L}_{\text{alg}}(\mathcal{S}, \mathbf{t}) = \mathcal{L}_{\text{alg}}(\tilde{\mathcal{S}}, \mathbf{t}) \quad \forall \tilde{\mathcal{S}} \in \{\mathcal{S}' \mid \mathbf{y}' \in \mathcal{B}_r(\mathbf{y})\}.$$

153 We will refer to  $\tilde{r}(\mathbf{t})$  as the certified radius for  $\mathbf{t}$ . A point-wise certificate then would be a lower  
 154 bound on the certified radius for a particular sample. The certificate is *exact* if it gives the true  
 155 certified radius  $\tilde{r}(\mathbf{t})$  rather than just a lower bound.

156 **Semi-Supervised Deep Partition Aggregation (SS-DPA).** Levine & Feizi (2020) introduce SS-  
 157 DPA, a framework that builds a certified defense against label-flipping poisoning attacks. The  
 158 framework certifies a partition aggregation ensemble  $g_{\mathcal{S}}$ , i.e., an ensemble consisting of  $N_p$  base  
 159 classifiers  $f_{\{1, \dots, N_p\}}$  trained on disjoint partitions  $P_{\{1, \dots, N_p\}}$  of the training data  $\mathcal{S}$ . The motivation  
 160 behind training on disjoint partitions is simple: Poisoning one label in the training data affects the  
 161 prediction of only one of the base-classifiers. The training data  $\mathcal{S}$  is first sorted without using the  
 labels and then partitioned based on the sorted order. This ensures that the partitioning is invariant

162 to any label poisoning attack. As the unlabeled data is trustworthy, we can make use of a self-  
 163 supervised learning algorithm to extract features from the entire unlabeled training data and train  
 164 each  $f_i$  using the extracted features and labels corresponding to  $P_i$ . At inference time, each base  
 165 classifier  $f_i$ , trained on its corresponding partition  $P_i$  of  $\mathcal{S}$  predicts the class for a given test sample  
 166  $\mathbf{t} \in \mathcal{T}$  as  $f_i(\mathbf{t}) \in [K]$ . The prediction of the ensemble  $g_{\mathcal{S}}(\mathbf{t})$  is then determined by a majority vote:  
 167  $g_{\mathcal{S}}(\mathbf{t}) = \arg \max_{c \in [K]} n_c(\mathbf{t})$ , where  $n_c(\mathbf{t}) := |\{i \in [N_p] \mid f_i(\mathbf{t}) = c\}|$  is the number of votes  
 168 received by class  $c$ . Ties are resolved deterministically by choosing the smaller index. If we denote  
 169  $g_{\mathcal{S}}(\mathbf{t})$  as  $c^*$ , the certificate  $\tilde{\rho}(\mathbf{t})$  for sample  $\mathbf{t}$  is given as:

$$170 \quad 171 \quad \tilde{\rho}(\mathbf{t}) := \left\lfloor \frac{n_{c^*}(\mathbf{t}) - \max_{c' \neq c^*} (n_{c'}(\mathbf{t}) + \mathbf{1}_{c' < c^*})}{2} \right\rfloor. \\ 172$$

173 The above guarantee says that for a poisoned dataset  $\tilde{\mathcal{S}}$  obtained by changing the labels of at most  $\tilde{\rho}$   
 174 samples in  $\mathcal{S}$ ,  $g_{\tilde{\mathcal{S}}}(\mathbf{t}) = c^*$ . As each base classifier is treated as a black-box, the certificate derivation  
 175 follows from a key worst-case assumption: **The prediction of a base classifier can be changed by**  
 176 **a single label flip**. The formal description of the worst case scenario is presented in App. A.1. With  
 177 *white-box* knowledge about the base classifiers, one can *improve* upon this worst-case assumption,  
 178 leading to a tighter certificate for the ensemble.  
 179

### 180 3 METHODOLOGY: ENSEMBLECERT AND SCALABELCERT

#### 181 3.1 ENSEMBLECERT

182 The underlying worst-case assumption in existing partition aggregation-based certificates, which  
 183 says that the prediction of a base classifiers can be changed with a single label flip, can be over-  
 184 come given that we have the following white-box information: for all base classifiers  $f_{\{1, \dots, N_p\}}$  and  
 185  $\forall c \in [K]$ , we have access to  $\rho_i^c$ , which is the minimum number of label flips in  $P_i$  required to change  
 186 the prediction of the base classifier  $f_i$  (trained on  $P_i$ ) to class  $c$ . Access to the white-box knowledge  
 187 through  $\rho_i^c$  enables verification of the worst-case assumption and provides the necessary information  
 188 to derive a tighter ensemble-level certificate. Note that the ensemble-level certificate  $\tilde{\rho}(\mathbf{t})$  that repre-  
 189 **sents the maximum number of flips upto which the ensemble prediction for a sample  $\mathbf{t}$  remains**  
 190 **unchanged**, is simply one less than the minimum number of flips required to change the ensemble  
 191 prediction. To determine the ensemble certificate  $\tilde{\rho}(\mathbf{t})$ , we first compute, for each class  $c$ , the least  
 192 number of flips needed to make  $c$  the majority class, and then take the minimum over all classes.  
 193

194 **Integer Program Formulation for Ensemble-wide Certification.** We denote the problem of find-  
 195 ing the minimum number of label flips in the training set required to change the prediction of the  
 196 ensemble to a particular class  $c'$  as  $P_1(c')$ . The white-box information  $\rho_i^c$  is collected in  $\rho \in \mathbb{R}^{N_p \times K}$ .  
 197 Given  $\rho$ , finding the optimal attack for the adversary, which is equivalent to solving  $P_1(c')$ , poses  
 198 as a combinatorial optimization problem leading to an Integer Program (IP) formulation of  $P_1(c')$ .  
 199 We denote the  $i$ th base classifier as  $f_i$  if trained on the clean data and  $\tilde{f}_i$  if trained on the per-  
 200 turbed data. The predictions from  $f_{\{1, \dots, N_p\}}$  and  $\tilde{f}_{\{1, \dots, N_p\}}$  on the sample  $\mathbf{t}$  are collected in the  
 201 vote configurations  $\mathbf{V}$  and  $\tilde{\mathbf{V}} \in \mathbb{R}^{N_p \times K}$  respectively:  $\forall i \in N_p, c \in [K] : v_i^c = \mathbf{1}\{f_i(\mathbf{t}) = c\}$ ,  
 202  $\tilde{v}_i^c = \mathbf{1}\{\tilde{f}_i(\mathbf{t}) = c\}$ . Note that  $\sum_{c=1}^K v_i^c = 1$  and  $\sum_{c=1}^K \tilde{v}_i^c = 1$  for all  $i \in [N_p]$ . Con-  
 203 cretely, to model  $P_1(c')$ , the number of label flips required to reach the vote configuration  $\tilde{\mathbf{V}}$  from  
 204  $\mathbf{V}$  is  $\sum_{i=1}^{N_p} \sum_{c=1}^K \rho_i^c \tilde{v}_i^c$ . The constraint that  $c'$  should be the majority class after adversarial ma-  
 205 nipulation of labels can be represented as  $\sum_{i=1}^{N_p} (\tilde{v}_i^{c'} - \tilde{v}_i^c) \geq \mathbf{1}_{c < c'}$ , for all  $c \neq c'$ . Recollect  
 206  $\sum_{c=1}^K \tilde{v}_i^c = 1$ ,  $\forall i \in [N_p]$  should also be satisfied. Thus, this gives the IP formulation of  $P_1(c')$ :  
 207

$$211 \quad 212 \quad P_1(c') : \min_{\tilde{\mathbf{V}}} \sum_{i=1}^{N_p} \sum_{c=1}^K \rho_i^c \tilde{v}_i^c \quad \text{s.t.} \quad \forall c \neq c' : \sum_{i=1}^{N_p} (\tilde{v}_i^{c'} - \tilde{v}_i^c) \geq \mathbf{1}_{c < c'}, \\ 213 \quad 214 \quad \forall i \in [N_p], \forall c \in [K] : \sum_{c=1}^K \tilde{v}_i^c = 1, \quad \tilde{v}_i^c \in \{0, 1\}.$$

216 The ensemble-level certificate  $\tilde{\rho}(\mathbf{t})$  for a test sample  $\mathbf{t}$  can then be derived, as mentioned in Sec. 3.1,  
 217 by simply subtracting one from the minimum over  $P_1(c)$ , that is,  $\tilde{\rho}(\mathbf{t}) = \min_{c \in [K] \setminus c^*} P_1(c) - 1$ .  
 218

219 **Reduction to Polynomial-time.** Solving  $P_1(c)$  in its current form is computationally prohibitive,  
 220 scaling as  $\mathcal{O}(2^{N_p} \times K)$  in the worst case. Thus, deriving  $\tilde{\rho}$  is even more expensive, with complexity  
 221  $\mathcal{O}(K \times 2^{N_p} \times K)$ . The problem becomes intractable even for small values of  $N_p$  and  $K$ , motivating  
 222 the need for a more tractable alternative. We denote as  $P_2(c')$ , a relaxation of  $P_1(c')$  that finds the  
 223 minimum number of label flips needed to make  $c'$  surpass *only*  $c^*$  (the original majority class) in the  
 224 number of votes, rather than making  $c'$  the overall majority class. The formulation of  $P_2(c')$  can be  
 225 obtained from  $P_1(c')$  by relaxing the constraint  $\sum_{i=1}^{N_p} (\tilde{v}_i^{c'} - \tilde{v}_i^c) \geq \mathbf{1}_{c < c'} \forall c \neq c'$  to the constraint  
 226  $(\tilde{v}_i^{c'} - \tilde{v}_i^{c^*}) \geq \mathbf{1}_{c^* < c'}$ . Despite this relaxation, we have the following result proved in App. A.2.  
 227

228 **Theorem 1** (Equivalence between problems  $P_1$  and  $P_2$ ).  
 229

$$\min_{c \in [K] \setminus c^*} P_1(c) = \min_{c \in [K] \setminus c^*} P_2(c)$$

231 The intuition for the above result is as follows: while trying to make  $c'$  surpass  $c^*$ , if another class  $c''$   
 232 becomes the majority class, then changing the ensemble prediction to  $c''$  should be easier compared  
 233 to  $c'$ . This result is particularly important, as we show that  $P_2(c)$  can be reduced to an instance of the  
 234 Multiple Choice Knapsack Problem (MCKP). Since MCKP is solvable in pseudopolynomial-time  
 235 (Dudzinski & Walukiewicz, 1987), our approach achieves a complexity of  $\mathcal{O}(N_p^2)$  for solving  $P_2$  per  
 236 class (App. A.2). Consequently, the ensemble-wide certificate  $\tilde{\rho}(\mathbf{t})$  can be computed in *polynomial*  
 237 time by solving  $P_2(c)$  for every class and finding the minimum, that is,  $\tilde{\rho}(\mathbf{t}) = \min_{c \in [K] \setminus c^*} P_2(c) -$   
 238 1. This represents a substantial improvement over the naive ILP formulation with complexity  $\mathcal{O}(K \times$   
 239  $2^{N_p} \times K)$ . We refer to App. A.3 for details on the reduction of  $P_2(c')$  to MCKP.  
 240

## 241 3.2 EXTRACTION OF WHITE-BOX KNOWLEDGE THROUGH SCALABELCERT

242 The approach of our white-box certificate *ScalabelCert* builds on the framework introduced by La-  
 243 belCert (Sabanayagam et al., 2025). LabelCert provides an exact certificate that determines whether  
 244 the model prediction remains unchanged when at most  $r$  training labels are flipped. This definition  
 245 of the certificate does not immediately align with the white-box knowledge that EnsembleCert util-  
 246 izes, which is the minimum number of label flips required to change the prediction of the classifier  
 247 to a *particular* class. Even more problematic, the computation of the certificate by LabelCert is  
 248 NP-hard and only scales to a few hundred labeled datapoints. ScalabelCert makes modifications to  
 249 the LabelCert approach to address these shortcomings, which result in the computation of an *exact*  
 250 certificate against label-flipping attacks in *polynomial* time. Next, we provide a brief overview of  
 251 the approach by LabelCert, and then introduce the developments leading to ScalabelCert.  
 252

253 **Infinite-Width Neural Networks and The Equivalence to Kernel Methods.** The Neural Tangent  
 254 Kernel (NTK) of a neural network  $f_\theta$  between two inputs  $i$  and  $j$  with features  $x_i$  and  $x_j$  is defined as  
 255  $Q_i^j = \mathbb{E}_\theta[\langle \nabla_\theta f_\theta(x_i), \nabla_\theta f_\theta(x_j) \rangle]$ , where the expectation is taken over the parameter initialization.  
 256 When  $f_\theta$  is an infinitely wide neural network, the dynamics of training  $f_\theta$  for a classification task  
 257 using a soft-margin loss are the same as those of an SVM with  $f_\theta$ 's NTK as kernel (Chen et al.,  
 258 2022). Similarly, if a regression loss (regularized mean-square) is used, the training dynamics are  
 259 equivalent to those of kernel regression using  $f_\theta$ 's NTK as kernel (Jacot et al., 2018).

260 **LabelCert.** For a test sample  $\mathbf{t}$ , LabelCert computes a point-wise certificate for sufficiently wide  
 261 neural networks, by deriving a certificate for a kernel SVM with  $f_\theta$ 's NTK as kernel, which—due  
 262 to the above equivalence—extends to a certificate for  $f_\theta$ . Recall that in the dual formulation of an  
 263 SVM, the parameters are the dual variables  $\alpha \in \mathbb{R}^n$  derived by solving the following problem:  
 264

$$P_{\text{svm}}(\mathbf{y}) = \min_{\alpha} - \sum_{i=1}^n \alpha_i + \frac{1}{2} \sum_{i=1}^n \sum_{j=1}^n \alpha_i \alpha_j y_i y_j Q_i^j \quad \text{s.t.} \quad 0 \leq \alpha_i \leq C, \forall i = [n]$$

265 where  $n$  is the number of training data,  $C$  is the regularization parameter that controls the trade-off  
 266 between maximizing the margin and minimizing classification error, and  $Q_i^j$  is the chosen kernel  
 267 between inputs  $i$  and  $j$ . Let the set of  $\alpha$  vectors solving  $P_{\text{svm}}(\mathbf{y})$  be  $\mathcal{S}(\mathbf{y})$ . The prediction for a test  
 268

sample  $\mathbf{t}$  is given by  $p_t = \text{sign}(\sum_{i=1}^n \alpha_i \tilde{y}_i Q_t^i)$ . Let  $\hat{p}_t$  be the prediction of the SVM trained using clean labels. The certificate is computed by converting the following problem  $P_{\text{cert}}(\mathbf{y})$  to a MILP:

$$P_{\text{cert}}(\mathbf{y}) := \min_{\tilde{\mathbf{y}}, \boldsymbol{\alpha}} \text{sign}(\hat{p}_t) \sum_{i=1}^n \alpha_i \tilde{y}_i Q_t^i \quad \text{s.t.} \quad \tilde{y} \in \mathcal{A}_r(\mathbf{y}), \quad \boldsymbol{\alpha} \in S(\tilde{\mathbf{y}})$$

Whether the model prediction for  $\mathbf{t}$  is robust up to  $r$  label flips or not is determined by the sign of the solution to  $P_{\text{cert}}(\mathbf{y})$ , with a positive sign indicating robustness.

**SVM Formulation for Sufficiently Small  $C$ .** The complexity of solving  $P_{\text{cert}}(\mathbf{y})$  comes largely from replacing the inner optimization problem  $\boldsymbol{\alpha} \in S(\tilde{\mathbf{y}})$  with the KKT (Karush-Kuhn-Tucker) conditions of  $P_{\text{svm}}(\mathbf{y})$ , which can be done as  $P_{\text{svm}}(\mathbf{y})$  is convex (Dempe & Dutta, 2012; Sabanayagam et al., 2025). We show that on using a sufficiently small  $C$ , we can entirely forego the inner optimization problem and convert  $P_{\text{cert}}(\mathbf{y})$  to a simpler, single-level problem based on Theorem 2.

**Theorem 2.** *Given a soft margin SVM with regularization  $C$ , kernel entry between training samples  $i, j$  as  $Q_i^j$ , and  $\boldsymbol{\alpha}$  being the solution to  $P_{\text{svm}}(\mathbf{y})$ , then if*

$$\max_{i \in [n]} \sum_{j \in [n]} |Q_i^j| \leq \frac{1}{C}, \quad \text{it follows that} \quad \forall \mathbf{y} \in \{-1, 1\}^n : \quad \boldsymbol{\alpha} = C \cdot \mathbf{1}^n$$

The proof is presented in App. A.4. When  $C$  satisfies the condition stated above, the alpha values are equal to  $C$  regardless of the labels. Thus, choosing  $C$  appropriately gives us the liberty to eliminate the inner optimization problem  $\boldsymbol{\alpha} \in S(\tilde{\mathbf{y}})$  as  $\boldsymbol{\alpha}$  is invariant to different labelings of the data. The SVM prediction in this case simplifies to  $p_t = \text{sign}(\sum_{i=1}^n C \tilde{y}_i Q_t^i)$ . As  $C$  is a positive constant, this further simplifies to  $p_t = \text{sign}(\sum_{i=1}^n \tilde{y}_i Q_t^i)$ . Integrating this insight into ScaLabelCert, we develop an efficient computation scheme for exact white-box certificates for infinite-width networks below that calculates the minimum number of label flips needed to change the prediction of the model.

**ScaLabelCert For The Binary Setting.** Our objective is to find the minimum number of label flips required to change the SVM prediction, i.e., to make  $\text{sign}(\hat{p}_t) \sum_{i=1}^n \alpha_i \tilde{y}_i Q_t^i$  negative. Under sufficiently small  $C$ , the above objective can be formulated as:

$$O_1(\mathbf{y}) : \min_{\tilde{\mathbf{y}} \in \{-1, 1\}^n} \frac{1}{2} \sum_{i=1}^n (1 - y_i \tilde{y}_i) \quad \text{s.t.} \quad \text{sign}(\hat{p}_t) \sum_{i=1}^n \tilde{y}_i Q_t^i < 0, \quad \forall i \in [n] : \tilde{y}_i \in \{-1, 1\}.$$

$O_1(\mathbf{y})$  can be solved in polynomial time (App. A.5). The intuition is that the labels corresponding to the largest positive contributions in  $\text{sign}(\hat{p}_t) (\sum_{i=1}^n y_i Q_t^i)$  are the most influential in determining the prediction, so flipping these labels greedily till the prediction changes is the optimal attack from the adversary's point of view. Thus, solving  $O_1(\mathbf{y})$  leads to a polynomial time computable exact certificate for sufficiently-wide neural networks, if  $f_\theta$ 's NTK is chosen as the SVM's kernel.

**ScaLabelCert For The Multi-Class Setting.** For the multi-class case, we use the one-vs-all strategy by decomposing the problem with  $K$  classes into  $K$  separate binary classification tasks. For each class  $c \in [K]$ , a binary classifier is trained to distinguish between samples of class  $c$  and samples from all other classes. Assume that  $p_c$  is the prediction score of a classifier for the learning problem corresponding to class  $c$ . Then, the class prediction  $c^*$  for a test sample is constructed by  $c^* = \arg \max_{c \in [K]} p_c$ . The labels are collected in the vector  $\mathbf{y}$  where  $\mathbf{y}_i^c = 1$  if the class of the  $i$ th sample is  $c$ , and 0 otherwise. Recall that for each base classifier, EnsembleCert requires white-box certificates that determine, for every class, the minimum number of label flips needed to change the model's prediction to that class. Using a soft-margin kernel SVM with a sufficiently small  $C$  as our base model, the certificate **computing minimum number of label flips required to change the prediction of the model to a particular class  $c'$**  can be formulated as (derived in App. A.6):

$$O_1(c') : \min_{\tilde{\mathbf{y}}} \sum_{i \in [N]} \left( 1 - \sum_{c \in [K]} y_i^c \tilde{y}_i^c \right) \quad \text{s.t.} \quad \sum_{i \in [N]} \tilde{y}_i^{c'} Q_t^i > \sum_{i \in [N]} \tilde{y}_i^c Q_t^i \quad \forall c \neq c', \\ \forall i \in [N], c \in [K] : \sum_{c \in [K]} \tilde{y}_i^c = 1, \quad \tilde{y}_i^c \in \{0, 1\}. \quad (1)$$

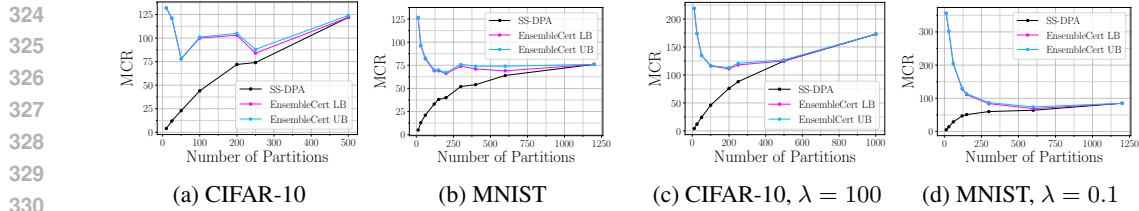


Figure 2: EnsembleCert evaluation using the NTK for (i) kernel SVM with a sufficiently small  $C$  (a, b); (ii) kernel regression under strong regularization (c, d). Median certified robustness either remains largely invariant across partitions or exhibits a decay until the white-box certificate converges to the black-box certificate. The tightness of our bounds on the *exact* certificate for the ensemble is evident, as the upper (EnsembleCert UB) and lower (EnsembleCert LB) bounds largely coincide across all plots.

While solving  $O_1(c')$  is NP-hard, we show that *tight lower and upper bounds* for the solution of  $O_1(c')$  can be computed in polynomial time (see App. A.7).

**Certificate for Kernel Regression.** With minor modifications, we can leverage the above formulation to certify a kernel regression model. Specifically, the adjustment is to replace  $Q_t^i$  with

$$(Q_{\text{eff}})_t^i = [(Q_{\text{train}} + \lambda I)^{-1} Q_{t,:}]_i$$

where  $Q_{\text{train}}$  is the kernel matrix for the training samples;  $Q_{t,:}$  is the vector of kernel entries for test sample  $t$  and the training samples; and  $\lambda$  is the regularization parameter. Deriving the certificate for kernel regression with the above modifications, we certify a sufficiently wide NN trained on a regularized mean-squared loss by using the network’s NTK as the kernel.

**Exact Certificate Given No Partitioning** ( $N_p = 1$ ). When there is no partitioning, we do not need to solve  $O_1(c')$  exactly for every  $c'$  to get an exact certificate for a stand-alone model. As  $O_1(c')$  represents the number of flips required to change the prediction to a particular class  $c'$ , the *exact* certificate for the stand-alone model can be derived by simply computing the *minimum* over  $O_1(c')$  i.e.,  $\tilde{\rho}(\mathbf{t}) = \min_{c \in [K] \setminus c^*} O_1(c) - 1$ . We show that with ScaLabelCert, this can be solved *in polynomial time*, by employing a similar line of argument as Theorem 1. The proof is presented in App. A.6. This results in the **first exact certificate** for neural networks against a poisoning attack that scales to common image benchmark datasets like MNIST or CIFAR-10.

## 4 EXPERIMENTS AND RESULTS

**Implementation Details.** We perform experiments on MNIST, CIFAR-10, and binary MNIST 1-vs-7. Following SS-DPA (Levine & Feizi, 2020), before training the base-classifiers we extract unsupervised features using RotNet (Gidaris et al., 2018) for MNIST and SimCLR (Chen et al., 2020) for CIFAR-10, using pretrained models from Levine & Feizi (2020). For the supervised training of base-classifiers, the extracted RotNet features for MNIST are used as input to an infinitely-wide convolutional network with a one convolutional layer and no pooling for supervised classification. For CIFAR-10, SimCLR features are fed to an infinitely-wide fully-connected network with one hidden layer and no non-linear activation. NTK computations are performed using the Google neural-tangents library (Novak et al., 2020). Using the NN-kernel equivalence (Sec. 3.2), the NTK is then used either with a kernel SVM for wide NNs trained on the soft-margin loss or with kernel regression for wide NNs trained on the regularized mean-squared loss. **On CIFAR-10, we evaluate EnsembleCert additionally on two different types of base classifiers (i) Finite-width networks and (ii) Smoothed linear classifiers. The relevant implementation details can be found in App. C.4 and App. B respectively.** Solving the MCKP for ensemble-level certificates as described in Sec. 3.1 is implemented using standard dynamic programming. The metrics used for evaluation are *certified accuracy*, with certified accuracy at  $r$  label flips being the fraction of test samples for which the model prediction is correct and robust up to  $r$  label flips; and *median certified robustness* (MCR), which denotes the number of label flips upto which the model prediction for 50% of the correctly classified samples is robust. **We provide further implementation details and certification runtimes in App. C.1.**

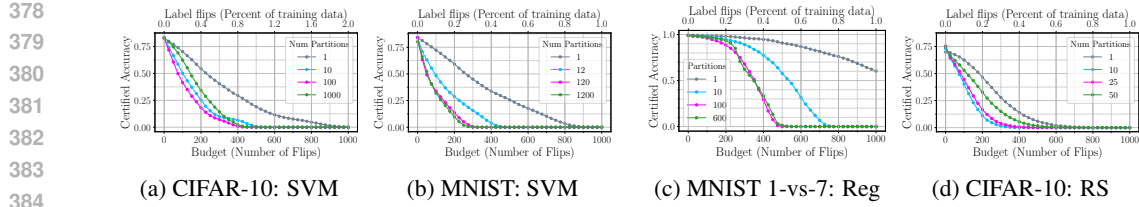


Figure 3: Comparing certified accuracies of stand-alone base models and their partition aggregation ensembles. Results with the base model as kernel SVM are in (a) and (b). (c): Using a stand-alone kernel regression model on MNIST 1-vs-7 maintains a certified accuracy of close to 80% when the certified accuracy for the corresponding best performing ensemble ( $N_p = 10$ ) reaches 0. (d): Smoothed linear regression as base model, comparing the stand-alone case and the ensembling.

**Experiments.** We instantiate EnsembleCert with sufficiently wide NNs trained on the soft-margin loss (equivalent to kernel SVMs with NTK) and the regularized mean square loss (equivalent to kernel ridge regression with NTK). Although regression losses may seem ill-suited for classification, they work well in practice (Mika et al., 1999; Rifkin et al., 2003). Moreover, Arora et al. (2019) showed that kernel ridge regression with the NTK of convolutional NNs achieves competitive performance on image datasets. As noted in our contributions, we additionally perform experiments on CIFAR-10 to evaluate EnsembleCert while using finite-width networks as base classifier. For base classifier certification in this case, we employ the gradient-based parameter bounding technique by Sosnin et al. (2024). The relevant details and plots can be found in App. C.4. We also evaluate EnsembleCert on CIFAR-10 using a smoothed linear regression model as the base classifier, certified via the smoothing-based method of Rosenfeld et al. (2020), which applies to smoothed linear models and yields analytic certificates without requiring the sampling process in randomized smoothing. The details of how we derive the necessary white-box knowledge for EnsembleCert by leveraging the smoothing approach can be found in the App. B. For every choice of base classifier, we observe that *injecting white-box knowledge into the ensemble substantially increases certified robustness for low to intermediate numbers of partitions*, highlighting the relative looseness of guarantees obtained using the black-box approach. The substantial improvement in certified robustness achieved by our white-box certificate for kernel methods as base classifiers is evident in Fig. 2. Further results demonstrating the same for every choice of base classifier can be found in App. C. The gap between the white-box and black-box certificates narrows as the number of partitions grows, with the white-box certificate eventually converging to the black-box certificate. This convergence reflects the realization of the worst-case scenario, where a single label flip can alter the prediction of a base classifier. Beyond the point of convergence, our method performs on par with the black-box approach. This behavior is a direct consequence of our method’s design and holds consistently across all experiments. In the next sections, we present some crucial insights that can be derived from our evaluation of EnsembleCert and ScaLabelCert.

**Invariance to Number of Partitions with Kernel SVM.** For the instantiation of EnsembleCert with kernel SVM, we use a regularization parameter  $C$  that is small enough to satisfy the condition in Theorem 2, as it is the key to computing scalable certificates for kernel SVM. We observe that the MCR of the white-box certificate remains largely **invariant to the number of partitions** for CIFAR-10 (Fig. 2a) and MNIST 1-vs-7 (Fig. 13a) until the point of convergence. On MNIST, there is a **sharp decline initially on increasing the number of partitions, followed by plateauing** (Fig. 2b). These findings indicate that strong guarantees can be achieved without requiring overly large ensembles.

**Robustness Decay with Kernel Regression.** For our instantiation of EnsembleCert with kernel ridge regression, we study the effect of the regularization parameter  $\lambda$  on certified robustness of the ensemble. For each dataset, we observe that the trend of certified robustness varies with the regularization parameter  $\lambda$ . As we increase  $\lambda$  from very small values, MCR initially improves with the number of partitions. Beyond a dataset-specific threshold, however, the trend reverses—**increasing the number of partitions leads to lower certified robustness**. For example, on CIFAR-10, when  $\lambda = 100$  (which lies beyond the threshold for this dataset), EnsembleCert certifies a median of 219 label flips with just 10 partitions, whereas using 1000 partitions reduces this to 173 (Fig. 2c). Similarly, on MNIST with  $\lambda = 0.1$ , EnsembleCert certifies 356 label flips using only 12 partitions, whereas using 1200 partitions lowers the certified robustness to 82 (Fig. 2d). We present plots for low values

432 of  $\lambda$  and discuss the behavioral change across the spectrum of  $\lambda$  in App. C.5. As robust kernel  
 433 regression is associated with the use of higher values of  $\lambda$  (Hu et al., 2021), the decreasing trend of the  
 434 MCR observed with high  $\lambda$  suggests that **deeper partitioning limits the true robustness potential**  
 435 of the ensemble when the underlying base classifier has a high degree of robustness.

436 **To Partition or Not to Partition?** The polynomial-time calculable exact certification method de-  
 437 rived by ScaLabelCert allows us to analyze the robustness of sufficiently wide neural networks  
 438 without employing an ensemble, that is,  $N_p = 1$ . While the simplification under small  $C$  eliminates  
 439 the need to calculate the training kernel for kernel SVM, making it easily scalable to datasets such  
 440 as CIFAR-10 and MNIST, it remains an essential component of the pipeline for kernel regression.  
 441 Thus, performing kernel regression on such datasets without partitioning is computationally chal-  
 442 lenging due to the need to compute the entire training kernel. Hence, in the no-partition setting,  
 443 we evaluate ScaLabelCert using the efficient kernel SVMs on all datasets and evaluate using kernel  
 444 regression only on the relatively small MNIST 1-vs-7 binary dataset. On CIFAR-10, ScaLabelCert  
 445 achieves non-trivial certified accuracy for up to 1000 label flips, which amounts to 2% of the train-  
 446 ing data Fig. 3a. In contrast, the evaluation by Levine & Feizi (2020) fails to certify *any* test sample  
 447 beyond 500 label flips. Additionally, we compare our method with the gradient-based parameter  
 448 bounding technique from Sosnin et al. (2024) and show that ScaLabelCert significantly outperforms  
 449 their method on CIFAR-10 in certified accuracy. Refer to App. C.3 for details. Motivated by the  
 450 observation that deeper partitioning may limit the ensemble’s true robustness potential, we further  
 451 investigate the role of partitioning by comparing the certified accuracy of a single base model against  
 452 that of its partition-aggregated ensemble. Our experiments across multiple datasets and base model  
 453 choices, as shown in Fig. 3, reveal that a **single base model trained on the entire training dataset**  
 454 **achieves significantly higher certified accuracy** as compared to its partition-aggregation ensemble.  
 455 This raises an important question: *Does partition aggregation enhance or diminish the robustness  
 456 potential of a given base model?*

## 457 5 DISCUSSION AND CONCLUSION

458 **Scarcity of relevant white-box certificates.** Our evaluations of EnsembleCert demonstrate signif-  
 459 icant improvement in certified robustness when the white-box knowledge of the base classifiers is  
 460 utilised. Notably, EnsembleCert demands white-box certificates deriving minimum number of sam-  
 461 ples that need to be tampered with to change the prediction to a particular class. The dearth in works  
 462 exploring certification of this nature pose an imminent challenge in the way of realising the true  
 463 potential of EnsembleCert.

464 **Certificate validity for finite-width neural networks.** ScaLabelCert leverages the equivalence  
 465 of infinite-width kernel methods with kernel methods induced by the NTK. This equivalence in  
 466 training dynamics and model outputs is exact only in the infinite-width case. For a finite-width neural  
 467 network however, where  $w$  denotes the smallest layer width of the network, the output difference of  
 468 the network to the SVM is bounded by  $\mathcal{O}\left(\frac{\ln w}{\sqrt{w}}\right)$  with probability  $p = 1 - \exp(-\Omega(w))$ , as shown  
 469 in Gosch et al. (2025), Liu et al. (2021). As  $w$  approaches infinity, the output difference approaches  
 470 0 and  $p$  approaches 1. Consequently, there must exist some width  $w'$  such that the output difference  
 471 between a network with width larger than  $w'$  and the corresponding kernel SVM is small enough for  
 472 the certificate to remain exact. To concretely compute  $w'$ , one would have to compute the constants  
 473 associated with the approximation error  $\mathcal{O}\left(\frac{\ln w}{\sqrt{w}}\right)$ . Unfortunately, the literature on the NTK so far is  
 474 mainly concerned with providing convergence statements in big- $\mathcal{O}$  notation and not with calculating  
 475 the individually involved constants. Hence, for a sufficiently wide network, the exact certificate  
 476 holds with probability  $p$  and does not apply with probability  $1 - p$ . Thus, our certificates obtained  
 477 by utilizing the neural network and NTK equivalence based on kernel SVM and regression represent  
 478 an asymptotically exact certificate as the width  $w$  approaches infinity.

479 **On Using Sufficiently Small  $C$  in Kernel SVM.** The choice of the parameter  $C$ , which controls  
 480 the penalty for misclassifications, introduces a robustness–accuracy trade-off in soft-margin SVMs.  
 481 Smaller values of  $C$  improve robustness to label noise and adversarial perturbations, as they en-  
 482 courage larger margins and reduce the influence of individual (potentially corrupted) points on the  
 483 decision boundary. Thus, our choice of  $C$  for the SVM simplification in Theorem 2 aligns with  
 484 building robust base-classifiers. Although this choice may not be optimal for clean accuracy, We

486 show that performance remains competitive. We ask the reader to refer to App. C.2 for a discussion  
 487 on the robustness-accuracy trade-off and the corresponding experiments.  
 488

489 **Versatility of ScaLabelCert.** Through the formulation  $O_1(c')$  (Eq. (1)), ScaLabelCert derives ef-  
 490 ficient certificates for sufficiently wide networks that compute the minimum number of label flips  
 491 needed to change the prediction of the classifier to a *particular* class  $c'$ . Although these certificates  
 492 are not exact, we compute sufficiently tight bounds (see Sec. 4). Note that the certificate definition  
 493 is different from the certified radius, which represents the minimum label flips needed to change  
 494 the classifier’s prediction to *any* class. We remind the reader that our certificate for computing the  
 495 certified radius for a stand-alone model is *exact* and *polynomial-time* calculable (App. A.6). More-  
 496 over, ScaLabelCert provides a general framework for certifying kernel SVMs and kernel regression  
 497 models against label-flipping. Using the NTK is one instance of this framework, enabling efficient  
 498 certification for sufficiently wide NNs. Finally, a kernel SVM with a sufficiently small  $C$  and kernel  
 499 regression-based classifiers can be interpreted as **weighted nearest-neighbor models**, where  $Q_t^i$  and  
 500  $(Q_{\text{eff}})_t^i$  denote the weight of the  $i$ th neighbor of the test sample  $t$  for kernel SVM and kernel regres-  
 501 sion, respectively. From this perspective, ScaLabelCert can also certify **weighted nearest-neighbor**  
**models** against label-flipping attacks in **polynomial time**, demonstrating its broad applicability.

502 **Potential of EnsembleCert for Certifying Against Clean-Label Attacks.** In this work, we util-  
 503 ize EnsembleCert to certify against label-flipping attacks. However, EnsembleCert can also lever-  
 504 age white-box knowledge of base-classifiers to provide robustness guarantees against **clean-label**  
 505 **attacks**. Specifically, consider an adversary capable of corrupting *only* the features of a training  
 506 sample within an  $\ell_p$  ball. Under this threat model, the white-box information  $\rho_i^c$  can denote the  
 507 number of samples that must be corrupted to change the prediction of the  $i$ th base classifier to class  
 508  $c$ . EnsembleCert can aggregate this white-box information from the base classifiers to compute the  
 509 number of samples in the *entire* training dataset that need to be corrupted to alter the prediction of  
 510 the ensemble. In this way, EnsembleCert can be adapted to derive white-box certificates for parti-  
 511 tion aggregation ensembles under multiple threat models. However, deriving efficient and scalable  
 512 white-box clean-label certificates for certifying the base classifiers is still an open challenge.  
 513

514 **Related Work.** Current ensemble-based poisoning certificates typically use the following ensem-  
 515 bling techniques: (i) randomized smoothing (Rosenfeld et al., 2020; Wang et al., 2020; Zhang et al.,  
 516 2022; Weber et al., 2023), where the randomization is over the training dataset, (ii) partition-based  
 517 aggregation (Levine & Feizi, 2020; Wang et al., 2022; Rezaei et al., 2023), and (iii) bootstrap ag-  
 518 gregation (Jia et al., 2021), where the base classifiers are trained on independently sampled subsets  
 519 of the training data. None of these works use white-box knowledge of the base classifiers, making  
 520 them inherently black-box methods. Apart from the white-box certificates discussed in the introduc-  
 521 tion (Sabanayagam et al., 2025; Sosnin et al., 2024), Gosch et al. (2025) is the only other white-box  
 522 certification method that certifies NNs against clean-label attacks, notably using the NTK approach  
 523 similar to ours and to Sabanayagam et al. (2025). The remaining white-box certificates in the litera-  
 524 ture do not extend to NNs and apply to only decision trees (Meyer et al., 2021; Drews et al., 2020),  
 525 nearest neighbor models (Jia et al., 2022) or naive Bayes classifiers (Bian et al., 2024).  
 526

527 **Conclusion.** We introduce **EnsembleCert**, a framework that leverages model information from  
 528 base-classifiers to yield significantly tighter ensemble-level certificates against label-flipping attacks  
 529 in *polynomial time*. To efficiently extract the white-box information, we develop **ScaLabelCert**, a  
 530 framework for the exact certification of sufficiently-wide NNs against label-flipping attacks. Sca-  
 531 labelCert computes exact certificates against label flipping attacks in polynomial time, making it the  
 532 *first polynomial-time* exact certification method that can certify (wide) NNs against data poison-  
 533 ing attacks. Through our evaluation of EnsembleCert instantiated with sufficiently wide NNs, we  
 534 observe that with robust base-classifiers, the partition aggregation ensemble can achieve stronger  
 535 guarantees using notably few partitions, outperforming excessively deep partitioning. This is cru-  
 536 cial, as excessively deep partitioning requires training a very large number of base-classifiers, in-  
 537 troducing significant computational overhead and limiting scalability. The experiments evaluating  
 538 ScaLabelCert on stand-alone models indicate that employing partition aggregation ensembles does  
 539 not always bring out the true robustness potential of the chosen base classifier architecture. Over-  
 540 all, our findings motivate the development of effective white-box certificates for finite-width neural  
 541 networks to bring out the true robustness of a partition aggregation ensemble and to understand the  
 542 role of partition-based ensembling itself in achieving strong robustness guarantees.

540 

## 6 ETHICS STATEMENT

541  
 542 Our work introduces EnsembleCert and ScaLabelCert, which, for the first time, leverage white-  
 543 box information to quantify the worst-case robustness of partition aggregation ensembles of neural  
 544 networks against label poisoning. Although such capabilities could, in principle, be misapplied by  
 545 adversaries, we contend that understanding these vulnerabilities is essential for the trustworthy and  
 546 safe use of neural networks. We therefore hold that the advantages of advancing robustness research  
 547 outweigh the potential downsides, and we do not anticipate any immediate risks arising from our  
 548 contributions. [Radhakrishnan et al. \(2022\)](#)

549 

## 550 7 REPRODUCIBILITY STATEMENT

551  
 552 The full codebase, along with configuration files for every experiment, is available at <https://figshare.com/s/f4ff623f9c47e63b8ef9>, which will be made public upon acceptance.

553 

## 554 REFERENCES

555  
 556 Sanjeev Arora, Simon S. Du, Wei Hu, Zhiyuan Li, Ruslan Salakhutdinov, and Ruosong Wang. On  
 557 exact computation with an infinitely wide neural net. In *Advances in Neural Information Processing  
 558 Systems*, volume 32, pp. 8139–8149, 2019. URL <https://proceedings.neurips.cc/paper/2019/hash/dbc4d84bfcfe2284ba11beffb853a8c4-Abstract.html>.

559  
 560 Hassan Ashtiani, Vinayak Pathak, and Ruth Urner. Black-box certification and learning under ad-  
 561 versarial perturbations. In Hal Daumé III and Aarti Singh (eds.), *Proceedings of the 37th Inter-  
 562 national Conference on Machine Learning*, volume 119 of *Proceedings of Machine Learning  
 563 Research*, pp. 388–398. PMLR, 2020. URL <https://proceedings.mlr.press/v119/ashtiani20a.html>.

564  
 565 Anish Athalye, Nicholas Carlini, and David Wagner. Obfuscated gradients give a false sense of se-  
 566 curity: Circumventing defenses to adversarial examples. In *International Conference on Machine  
 567 Learning (ICML)*, pp. 274–283, 2018.

568  
 569 Melis Ilayda Bal, Volkan Cevher, and Michael Muehlebach. Adversarial training for defense against  
 570 label poisoning attacks, 2025. URL <https://arxiv.org/abs/2502.17121>.

571  
 572 Song Bian, Xiating Ouyang, Zhiwei Fan, and Paraschos Koutris. Naive bayes classifiers over miss-  
 573 ing data: Decision and poisoning. In *Proceedings of the 41st International Conference on Ma-  
 574 chine Learning (ICML / PMLR)*, volume 235, pp. 3913–3934, 2024.

575  
 576 Battista Biggio, Blaine Nelson, and Pavel Laskov. Support vector machines under adversarial label  
 577 noise. In *Proceedings of the 3rd Asian Conference on Machine Learning, ACML 2011, Taoyuan,  
 578 Taiwan, November 13-15, 2011*, JMLR Proceedings, 2011. URL <http://proceedings.mlr.press/v20/biggio11/biggio11.pdf>.

579  
 580 Nicholas Carlini and David Wagner. Towards evaluating the robustness of neural networks. In *IEEE  
 581 Symposium on Security and Privacy (S&P)*, pp. 39–57, 2017.

582  
 583 Ting Chen, Simon Kornblith, Mohammad Norouzi, and Geoffrey Hinton. A simple framework for  
 584 contrastive learning of visual representations. In *International Conference on Machine Learning  
 585 (ICML)*, pp. 1597–1607. PMLR, 2020.

586  
 587 Yilan Chen, Wei Huang, Lam M. Nguyen, and Tsui-Wei Weng. On the equivalence between neu-  
 588 ral network and support vector machine, 2022. URL <https://arxiv.org/abs/2111.06063>.

589  
 590 Stephan Dempe and Joydeep Dutta. Is bilevel programming a special case of a mathematical pro-  
 591 gram with complementarity constraints? *Mathematical Programming*, 131(1):37–48, 2012.

592  
 593 Samuel Drews, Aws Albarghouthi, and Loris D’Antoni. Proving data-poisoning robustness in de-  
 594 cision trees. In *Proceedings of the 41st ACM SIGPLAN Conference on Programming Language  
 595 Design and Implementation (PLDI)*, pp. 1083–1097, 2020. doi: 10.1145/3385412.3385975.

594 Kazimierz Duddzinski and Stanislaw Walukiewicz. Exact methods for the knapsack problem and its  
 595 generalizations. *European Journal of Operational Research*, 28(1):3–21, 1987. doi: 10.1016/0377-2217(87)90165-2.

596

597 Spyros Gidaris, Praveer Singh, and Nikos Komodakis. Unsupervised representation learning by  
 598 predicting image rotations. In *International Conference on Learning Representations (ICLR)*,  
 599 2018.

600

601 Lukas Gosch, Mahalakshmi Sabanayagam, Debarghya Ghoshdastidar, and Stephan Günnemann.  
 602 Provable robustness of (graph) neural networks against data poisoning and backdoor attacks.  
 603 *Transactions on Machine Learning Research*, 2025-June, 2025. Accepted / Published in TMLR.

604

605 Tianyang Hu, Wenjia Wang, Cong Lin, and Guang Cheng. Regularization matters: A nonparamet-  
 606 ric perspective on overparametrized neural network. In *Proceedings of The 24th International  
 607 Conference on Artificial Intelligence and Statistics (AISTATS)*, volume 130, pp. 829–837. PMLR,  
 608 2021. URL <https://proceedings.mlr.press/v130/hu21a.html>.

609

610 Arthur Jacot, Franck Gabriel, and Clément Hongler. Neural tangent kernel: Convergence and gener-  
 611 alization in neural networks. In *Advances in Neural Information Processing Systems*, volume 31,  
 612 pp. 8571–8580, 2018.

613

614 Jinyuan Jia, Xiaoyu Cao, and Neil Zhenqiang Gong. Intrinsic certified robustness of bagging against  
 615 data poisoning attacks. In *Proceedings of the AAAI Conference on Artificial Intelligence*, vol-  
 616 ume 35, pp. 7961–7969, 2021. doi: 10.1609/aaai.v35i9.16971.

617

618 Jinyuan Jia, Yupei Liu, Xiaoyu Cao, and Neil Zhenqiang Gong. Certified robustness of nearest  
 619 neighbors against data poisoning and backdoor attacks. In *Proceedings of the 36th AAAI Confer-  
 620 ence on Artificial Intelligence (AAAI)*, pp. 9575–9583, 2022. doi: 10.1609/aaai.v36i9.21191.

621

622 Pang Wei Koh, Jacob Steinhardt, and Percy Liang. Stronger data poisoning attacks break data  
 623 sanitization defenses. *Machine Learning*, 111(1):1–47, 2021. doi: 10.1007/s10994-021-06119-y.

624

625 Alexander Levine and Soheil Feizi. Deep partition aggregation: Provable defense against general  
 626 poisoning attacks. *arXiv preprint arXiv:2006.14768*, 2020.

627

628 Chaoyue Liu, Libin Zhu, and Mikhail Belkin. On the linearity of large non-linear models: when and  
 629 why the tangent kernel is constant, 2021. URL <https://arxiv.org/abs/2010.01092>.

630

631 Anna P. Meyer, Aws Albarghouthi, and Loris D’Antoni. Certifying robustness to programmable  
 632 data bias in decision trees. In *Advances in Neural Information Processing Systems (NeurIPS)*, pp.  
 633 26276–26288, 2021.

634

635 S. Mika, G. Rätsch, J. Weston, B. Schölkopf, and K. R. Müller. Fisher discriminant analysis with  
 636 kernels. In *Proceedings of the 1999 IEEE Signal Processing Society Workshop on Neural Net-  
 637 works for Signal Processing (NNSP’99)*, pp. 41–48, 1999. doi: 10.1109/NNSP.1999.788121.

638

639 Roman Novak, Lechao Xiao, Jiri Hron, Jaehoon Lee, Alexander A. Alemi, Jascha Sohl-Dickstein,  
 640 and Samuel S. Schoenholz. Neural tangents: Fast and easy infinite neural networks in python. In  
 641 *International Conference on Learning Representations*, 2020. URL <https://github.com/google/neural-tangents>.

642

643 Andrea Paudice, Luis Muñoz-González, Andras Gyorgy, and Emil C Lupu. Label sanitization  
 644 against label flipping poisoning attacks. In *Joint European Conference on Machine Learning  
 645 and Knowledge Discovery in Databases*, pp. 5–15. Springer, 2018.

646

647 Adityanarayanan Radhakrishnan, George Stefanakis, Mikhail Belkin, and Caroline Uhler. Simple,  
 648 fast, and flexible framework for matrix completion with infinite width neural networks. *Pro-  
 649 ceedings of the National Academy of Sciences*, 119(16), April 2022. ISSN 1091-6490. doi:  
 650 10.1073/pnas.2115064119. URL <http://dx.doi.org/10.1073/pnas.2115064119>.

651

652 Keivan Rezaei, Kiarash Banihashem, Atoosa Chegini, and Soheil Feizi. Run-off election: Improved  
 653 provable defense against data poisoning attacks. In *Proceedings of the 40th International Confer-  
 654 ence on Machine Learning (ICML)*, 2023. URL <https://arxiv.org/abs/2302.02300>.

648 Ryan Rifkin, Gene Yeo, and Tomaso Poggio. Regularized least-squares classification. Technical Re-  
 649 port MIT-CSAIL-TR-2003-110, MIT Artificial Intelligence Laboratory and Center for Biological  
 650 and Computational Learning, 2003. URL [https://www.cs.toronto.edu/~urtasun/](https://www.cs.toronto.edu/~urtasun/courses/CSC411/tutorials/Rifkin.pdf)  
 651 [courses/CSC411/tutorials/Rifkin.pdf](https://www.cs.toronto.edu/~urtasun/courses/CSC411/tutorials/Rifkin.pdf).

652 Elan Rosenfeld, Ezra Winston, Pradeep Ravikumar, and Zico Kolter. Certified robustness to label-  
 653 flipping attacks via randomized smoothing. *arXiv preprint arXiv:2002.03018*, 2020.

654 Mahalakshmi Sabanayagam, Pascal Mattia Esser, and Debarghya Ghoshdastidar. Analysis of con-  
 655volutions, non-linearity and depth in graph neural networks using neural tangent kernel. *Trans-  
 656actions on Machine Learning Research*, 2023. URL [https://openreview.net/forum?](https://openreview.net/forum?id=xgYgDEof29)  
 657 [id=xgYgDEof29](https://openreview.net/forum?id=xgYgDEof29).

658 Mahalakshmi Sabanayagam, Lukas Gosch, Stephan Günemann, and Debarghya Ghoshdastidar.  
 659 Exact certification of (graph) neural networks against label poisoning, 2025. URL <https://arxiv.org/abs/2412.00537>.

660 Philip Sosnin, Mark N. Müller, Maximilian Baader, Calvin Tsay, and Matthew Wicker. Certified  
 661 robustness to data poisoning in gradient-based training. *arXiv preprint arXiv:2406.05670*, 2024.  
 662 v2.

663 Binghui Wang, Xiaoyu Cao, Jinyuan jia, and Neil Zhenqiang Gong. On certifying robustness against  
 664 backdoor attacks via randomized smoothing, 2020. URL <https://arxiv.org/abs/2002.11750>.

665 Wenxiao Wang, Alexander J Levine, and Soheil Feizi. Improved certified defenses against data  
 666 poisoning with (deterministic) finite aggregation. In *Proceedings of the 39th International Con-  
 667ference on Machine Learning (ICML)*, pp. 22769–22783, 2022. URL [https://arxiv.org/](https://arxiv.org/abs/2202.02628)  
 668 [abs/2202.02628](https://arxiv.org/abs/2202.02628).

669 Maurice Weber, Xiaojun Xu, Bojan Karlaš, Ce Zhang, and Bo Li. Rab: Provable robustness against  
 670 backdoor attacks. In *Proceedings of the IEEE Symposium on Security and Privacy (SP)*, 2023.  
 671 doi: 10.1109/SP46215.2023.10179451. *arXiv preprint arXiv:2003.08904* (initial preprint).

672 Han Xiao, Battista Biggio, Gavin Brown, Giorgio Fumera, Claudia Eckert, and Fabio Roli. Adver-  
 673sarial label flips attack on support vector machines. In *20th European Conference on Artificial  
 674 Intelligence (ECAI)*, pp. 870–875. IOS Press, 2015.

675 Yuhao Zhang, Aws Albarghouthi, and Loris D’Antoni. Bagflip: A certified defense against data  
 676 poisoning. In *Proceedings of NeurIPS (Advances in Neural Information Processing Systems)*,  
 677 2022. *arXiv:2205.13634 / NeurIPS 2022*.

678  
 679  
 680  
 681  
 682  
 683  
 684  
 685  
 686  
 687  
 688  
 689  
 690  
 691  
 692  
 693  
 694  
 695  
 696  
 697  
 698  
 699  
 700  
 701

702 A THEORETICAL DETAILS  
703704 A.1 THE FORMAL DESCRIPTION OF THE WORST CASE SCENARIO  
705

706 Recall that the prediction of the partition aggregation ensemble  $g_S(\mathbf{t})$  is determined by a major-  
707 ity vote over the prediction by the base classifiers  $f_{\{1, \dots, N_p\}}$ :  $g_S(\mathbf{t}) = \arg \max_{c \in [K]} n_c(\mathbf{t})$ , where  
708  $n_c(\mathbf{t}) := |\{i \in [N_p] \mid f_i(\mathbf{t}) = c\}|$  is the number of votes received by class  $c$ . Ties are resolved deter-  
709 ministically by choosing the smaller index. If we denote  $g_S(\mathbf{t})$  as  $c^*$ , the certificate  $\tilde{\rho}(\mathbf{t})$  for sample  
710  $\mathbf{t}$ , that computes the number of adversarial label flips upto which the prediction of the ensemble will  
711 not change, as derived by black-box treatment of the base classifier is given as:

$$712 \tilde{\rho}(\mathbf{t}) := \left\lfloor \frac{n_{c^*}(\mathbf{t}) - \max_{c' \neq c^*} (n_{c'}(\mathbf{t}) + \mathbf{1}_{c' < c^*})}{2} \right\rfloor. \\ 713$$

714 As each base classifier is treated as a black box, the certificate derivation follows from a key worst-  
715 case assumption: **The prediction of certain base classifiers can be altered by a single label flip**.  
716 The formal description of the worst-case scenario is given below.

717 **Formalising the worst-case scenario:** Let  $\mathcal{C}_{\text{sec}} := \arg \max_{c \neq c^*} (n_c(\mathbf{t}) + \mathbf{1}_{c < c^*})$ . One can think of  
718  $\mathcal{C}_{\text{sec}}$  as the set of runner-up classes. We define  $\mathcal{P}_{\text{maj}}$  as the set of base classifiers that voted for  $c^*$ .  
719 The worst-case scenario can be represented as:

720  $\exists c' \in \mathcal{C}_{\text{sec}} \text{ s.t. the prediction of at least } \tilde{\rho} + 1 \text{ base classifiers in } \mathcal{P}_{\text{maj}} \text{ can be changed from } c^* \text{ to } c'$   
721  $\text{with one label flip in their corresponding partitions. In such a scenario, attacking the corresponding}$   
722  $\text{base classifiers with one label flip each would change the prediction of the ensemble to } c'$ .

723 Note that the numerator in  $\tilde{\rho}$ :  $n_{c^*} - \max_{c' \neq c^*} (n_{c'}(\mathbf{t}) + \mathbf{1}_{c' < c^*})$ , is the difference in the number  
724 of the votes received by the majority class  $c^*$  and  $c'$ . Flipping the vote of a base classifier from  
725  $c^*$  to  $c'$  bridges the gap between  $c^*$  and  $c'$  by 2 votes, explaining the 2 in the denominator. In  
726 light of the worst-case assumption, the reader can now see that the certificate actually calculates  
727 the number of base classifiers whose prediction needs to be flipped in order to change the ensemble  
728 prediction. With *white-box* knowledge about the base classifiers, we can improve upon the worst-  
729 case assumption, leading to a tighter certificate for the ensemble. One could argue that we need  
730 the *white-box* information solely about the base classifiers in  $\mathcal{P}_{\text{maj}}$  and classes in  $\mathcal{C}_{\text{sec}}$  to challenge  
731 the assumption. The point to note is that if information about  $\mathcal{P}_{\text{maj}}$  indicates that the worst-case  
732 scenario cannot be realized, we cannot assume that the adversary will attack partitions only in  $\mathcal{P}_{\text{maj}}$   
733 and change the prediction to a class in  $\mathcal{C}_{\text{sec}}$ . Hence, to derive a tighter certificate, we would need this  
734 information for all base classifiers and classes.

735  
736 A.2 THEOREM 1:  $\min P_1(c) = \min P_2(c)$   
737

738 **Intuition.** Recall that  $P_1(c')$  denotes the minimum number of label flips needed to make  $c'$  the  
739 *majority class*, whereas  $P_2(c')$  denotes the minimum number of label flips needed to make  $c'$  surpass  
740 the current majority class  $c^*$  in number of votes. Intuitively, if  $c'$  is the class that requires the fewest  
741 flips to become the new prediction, then making it just beat  $c^*$  will already make it the majority  
742 class.

743 **Vote Configuration** Let  $\tilde{\mathbf{V}} \in \{0, 1\}^{N_p \times K}$  denote the perturbed vote configuration, where  $\tilde{v}_i^c =$   
744 1 if partition  $i$  votes for class  $c$  after label flips, and 0 otherwise. Let  $\mathbf{V}$  denote the clean vote  
745 configuration. We define  $O(\tilde{\mathbf{V}})$  as the number of label flips required to reach configuration  $\tilde{\mathbf{V}}$   
746 starting from the clean configuration  $\mathbf{V}$ .

747 **Restatement of  $P_1(c')$ .** Recall that  $P_1(c')$  is defined as the minimum number of label flips needed  
748 to make  $c'$  the majority class. In Sec. 3.1, the constraint was formulated through the set of inequalities

$$749 \sum_{i=1}^{N_p} (\tilde{v}_i^{c'} - \tilde{v}_i^c) \geq \mathbf{1}_{c < c'}, \quad \forall c \neq c', \\ 750$$

751 which constraints  $c'$  to be the majority class (with deterministic tie-breaking). For brevity, we  
752 now re-express this condition using the function  $\text{majVote}(\tilde{\mathbf{V}}) := \arg \max_{c \in [K]} \sum_{i=1}^{N_p} \tilde{v}_i^c$ , as  $c' =$   
753  $\text{majVote}(\tilde{\mathbf{V}})$  where ties are resolved deterministically by choosing the class with the smaller index.

756 With this shorthand notation, we write  
 757

$$\begin{aligned}
 758 \quad P_1(c') &= \min_{\tilde{\mathbf{V}}} O(\tilde{\mathbf{V}}) \\
 759 \\
 760 \quad \text{s.t.} \quad c' &= \text{majVote}(\tilde{\mathbf{V}}), \\
 761 \\
 762 \quad \sum_{c=1}^K \tilde{v}_i^c &= 1, \quad \forall i \in [N_p], \\
 763 \\
 764 \quad \tilde{v}_i^c \in \{0, 1\}, \quad \forall i \in [N_p], \forall c \in [K].
 765
 \end{aligned}$$

766 **Restatement of  $P_2(c')$ .** Problem  $P_2(c')$  relaxes the above by requiring  $c'$  to surpass *only* the original  
 767 majority class  $c^*$ , instead of all classes:  
 768

$$\begin{aligned}
 769 \quad P_2(c') &= \min_{\tilde{\mathbf{V}}} O(\tilde{\mathbf{V}}) \\
 770 \\
 771 \quad \text{s.t.} \quad \sum_{i=1}^{N_p} \left( \tilde{v}_i^{c'} - \tilde{v}_i^{c^*} \right) &\geq \mathbf{1}_{c^* < c'}, \\
 772 \\
 773 \quad \sum_{c=1}^K \tilde{v}_i^c &= 1, \quad \forall i \in [N_p], \\
 774 \\
 775 \quad \tilde{v}_i^c \in \{0, 1\}, \quad \forall i \in [N_p], \forall c \in [K].
 776
 \end{aligned}$$

777  
 778 **Theorem** (Restating Theorem 1).  $\min_{c' \in [K] \setminus \{c^*\}} P_1(c') = \min_{c' \in [K] \setminus \{c^*\}} P_2(c')$   
 779

780 *Proof.* We first state three lemmas and then combine them to prove the theorem.  
 781

782 **Lemma 1.**  $\forall c' \in [K] \setminus c^*, \quad P_1(c') \geq P_2(c')$ .  
 783

784 *Proof.* The feasible region of  $P_1(c')$  is contained within that of  $P_2(c')$  since the latter has a weaker  
 785 constraint. Hence,  $P_2(c')$  can only be smaller (or equal) to  $P_1(c')$ .  $\square$   
 786

787 **Lemma 2.**  $\forall c_1^* \in \arg \min_{c' \in [K] \setminus c^*} P_1(c'), \quad P_1(c_1^*) = P_2(c_1^*)$ .  
 788

789 *Proof.* By contradiction. Suppose  $P_1(c_1^*) > P_2(c_1^*)$ . Let  $\tilde{\mathbf{S}}$  be the optimal solution for  $P_2(c_1^*)$ , i.e.,  
 790

$$O(\tilde{\mathbf{S}}) = P_2(c_1^*). \quad (2)$$

791 Since  $O(\tilde{\mathbf{S}}) < P_1(c_1^*)$ ,  $\tilde{\mathbf{S}}$  is not feasible for  $P_1(c_1^*)$ . As the feasibility for  $P_1(c_1^*)$  requires  $c^*$  to be  
 792 the majority class, there must exist some  $c_s^* \neq c_1^*$  such that  $c_s^* = \text{majVote}(\tilde{\mathbf{S}})$ . Note that  $\tilde{\mathbf{S}}$  is feasible  
 793 for  $P_1(c_s^*)$  as  $c_s^*$  is the majority class for the vote configuration  $(\tilde{\mathbf{S}})$ , so

$$O(\tilde{\mathbf{S}}) \geq P_1(c_s^*). \quad (3)$$

794 Combining (2) and (3) with the assumption that  $P_1(c_1^*) > P_2(c_1^*)$  gives  $P_1(c_1^*) > P_1(c_s^*)$ , contra-  
 795 dicting the assumption that  $c_1^*$  minimizes  $P_1(c')$ .  $\square$   
 796

797 **Lemma 3.**  $\exists z^* \in \arg \min_{c' \in [K] \setminus c^*} P_2(c') \text{ such that } P_1(z^*) = P_2(z^*)$ .  
 798

799 *Proof.* Let  $c_2^* \in \arg \min_{c' \in [K] \setminus c^*} P_2(c')$  and let  $\tilde{\mathbf{S}}$  be the vote configuration in the optimal solution  
 800 for  $P_2(c_2^*)$ , i.e.,  
 801

$$O(\tilde{\mathbf{S}}) = P_2(c_2^*). \quad (4)$$

Let  $z^* = \text{majVote}(\tilde{\mathbf{S}})$ . Then  $\tilde{\mathbf{S}}$  is feasible for both  $P_1(z^*)$ , that requires  $z^*$  to be the majority class and  $P_2(z^*)$ , that requires  $z^*$  to have higher votes than  $c^*$ , implying

$$O(\tilde{\mathbf{S}}) \geq P_2(z^*) \quad \text{and} \quad (5)$$

$$O(\tilde{\mathbf{S}}) \geq P_1(z^*). \quad (6)$$

With (4), (5) and the minimality of  $c_2^*$ , we have  $z^* \in \arg \min_{c' \in [K] \setminus c^*} P_2(c')$  and  $O(\tilde{\mathbf{S}}) = P_2(z^*)$ . Combining this result with (6) and using Lemma 1.1 we conclude  $P_1(z^*) = P_2(z^*)$ .  $\square$

**Proof of Theorem 1.** Let  $c_1^* \in \arg \min_{c' \in [K] \setminus c^*} P_1(c')$  and  $z^* \in \arg \min_{c' \in [K] \setminus c^*} P_2(c')$  s.t.  $P_1(z^*) = P_2(z^*)$ . Using Lemmas 1.2 and 1.3, we obtain

$$P_1(z^*) = P_2(z^*) \leq P_2(c_1^*) = P_1(c_1^*),$$

which implies

$$P_1(c_1^*) = P_1(z^*) = P_2(z^*),$$

thus proving that

$$\boxed{\min_{c' \in [K] \setminus \{c^*\}} P_1(c') = \min_{c' \in [K] \setminus \{c^*\}} P_2(c')}.$$

$\square$

### A.3 REDUCTION TO MCKP AND COMPLEXITY ANALYSIS

In this section, we will use the terms base classifiers and partitions interchangeably, and discuss the optimal attack from an adversary's point of view to make  $c'$  surpass  $c^*$ . Let's denote the set of partitions that voted for  $c^*$  originally as  $\mathcal{P}_{\text{maj}}$ , the ones that voted for  $c'$  originally as  $\mathcal{P}_{\text{target}}$  and rest of the partitions as  $\mathcal{P}_{\text{rest}}$ . Formally:

$$\mathcal{P}_{\text{maj}} = \{i \in [N_p] \mid v_i^{c^*} = 1\}, \quad \mathcal{P}_{\text{target}} = \{i \in [N_p] \mid v_i^{c'} = 1\}, \quad \mathcal{P}_{\text{rest}} = [N_p] \setminus (\mathcal{P}_{\text{target}} \cup \mathcal{P}_{\text{maj}}).$$

The adversary will not attack partitions in  $\mathcal{P}_{\text{target}}$ . If a partition in  $\mathcal{P}_{\text{rest}}$  is attacked, the vote can change only to  $c'$ . Changing the vote to any other class will deem the label perturbation pointless. Let  $\mathcal{C}_i$  be the set of classes that partition  $i$  could vote for after the optimal attack:

$$\forall i \in \mathcal{P}_{\text{rest}} : \mathcal{C}_i = \{c \in K \mid c = c' \text{ or } v_i^c = 1\}, \quad \forall i \in \mathcal{P}_{\text{target}} : \mathcal{C}_i = \{c'\}.$$

Note that  $\forall i \in [N_p]$ , we need the binary variable  $\tilde{v}_i^c$  only if  $c \in \mathcal{C}_i$ . Attacking a partition in  $\mathcal{P}_{\text{maj}}$  could change the vote to  $c'$  or to the class with the minimal number of flips required for a prediction change to that class. Formalizing the above notion, we define  $c_{\min}$  as:  $\forall i \in \mathcal{P}_{\text{maj}} : c_{\min}(i) = \arg \min_{c \in [K] \setminus c^*} \rho_i^c$ . Given this we have:

$$\forall i \in \mathcal{P}_{\text{maj}} : \mathcal{C}_i = \{c \in K \mid c = c' \text{ or } c = c_{\min}(i) \text{ or } c = c^*\}.$$

We model the constraint  $C_1 := \sum_{i=1}^{N_p} (\tilde{v}_i^{c'} - \tilde{v}_i^{c^*}) \geq \mathbf{1}_{c^* < c'}$  differently. Let  $d$  be the original difference between the number of votes for  $c'$  and  $c^*$ :  $d = \sum_{i=1}^{N_p} (v_i^{c^*} - v_i^{c'})$ . We define  $r_i^c$  to be the reduction in the gap between  $c'$  and  $c^*$  caused by flipping the vote of partition  $i$  to class  $c$ . For partitions in  $\mathcal{P}_{\text{maj}}$ , if the vote changes to  $c'$ , the difference will decrease by 2. If the vote goes to any other class, the reduction is by 1. It is trivial to see that  $\forall i \in \mathcal{P}_{\text{target}}, c \in \mathcal{C}_i : r_i^c = 0$ . We can similarly define these values for partitions in  $\mathcal{P}_{\text{rest}}$  and get:

$$\forall i \in \mathcal{P}_{\text{maj}}, c \in \mathcal{C}_i : r_i^c = \begin{cases} 2 & \text{if } c = c' \\ 1 & \text{else if } c = c_{\min}(i) \\ 0 & \text{else if } c = c^* \end{cases}, \quad \forall i \in \mathcal{P}_{\text{rest}}, c \in \mathcal{C}_i : r_i^c = \begin{cases} 1 & \text{if } c = c' \\ 0 & \text{else} \end{cases}$$

For  $c'$  to have higher number of votes than  $c^*$ , the total reduction in the difference should be greater than or equal to  $d + \mathbf{1}_{c^* < c'}$ . Remodeling  $C_1$  with the above idea, we can reformulate  $P_2(c')$  as:

864

$$\begin{aligned}
865 \quad P_2(c') : \quad \min_{\tilde{\mathbf{V}}} \sum_{i=1}^{N_p} \sum_{c \in C_i} \rho_i^c \tilde{v}_i^c \quad \text{s.t.} \quad \sum_{i=1}^{N_p} \sum_{c \in C_i} r_i^c \tilde{v}_i^c \geq d + \mathbf{1}_{c^* < c'}, \\
866 \quad \forall i \in [N_p], \forall c \in C_i : \quad \sum_{c \in C_i} \tilde{v}_i^c = 1, \quad \tilde{v}_i^c \in \{0, 1\}.
\end{aligned}$$

870

This problem can be easily converted to a MCKP (multiple choice knapsack problem). To arrive at the exact formulation of MCKP, we need to change the min objective to a max objective and reverse the sign of the constraint inequality. Note that solving  $\min_{\tilde{v}} O(\tilde{\mathbf{V}})$  is same as solving  $A - \max_{\tilde{v}} (A - O(\tilde{\mathbf{V}}))$ , where  $A$  is a positive constant. We choose the constant  $A$  to be  $N_p * \rho_{\max}$ , where  $\rho_{\max} = \max_{i \in N_p, c \in C_i} \rho_i^c$ . Lets denote  $P_3(c')$  as follows .

876

$$\begin{aligned}
877 \quad P_3(c') = \max_{\tilde{v}} (N_p * \rho_{\max} - \sum_{i=1}^{N_p} \sum_{c \in C_i} \rho_i^c \tilde{v}_i^c) \\
878 \quad \text{s.t.} \quad (\sum_{i=0}^{N_p-1} \sum_{c \in C_i} r_i^c \tilde{v}_i^c) \geq d + \mathbf{1}_{c^* < c'}, \\
879 \quad \sum_{c \in C_i} \tilde{v}_i^c = 1, \quad \forall i \in [N_p], \\
880 \quad \tilde{v}_i^c \in \{0, 1\}, \quad \forall i \in [N_p], \forall c \in C_i
\end{aligned}$$

887

As  $\sum_{c \in C_i} \tilde{v}_i^c = 1$ , we can rewrite  $N_p * \rho_{\max}$  as  $(\sum_{i=0}^{N_p-1} \sum_{c \in C_i} \rho_{\max} * \tilde{v}_i^c)$ . Using this trick, we reformulate  $P_3(c')$  as :

890

$$\begin{aligned}
891 \quad P_3(c') = \max_{\tilde{v}} \sum_{i=1}^{N_p} \sum_{c \in C_i} (\rho_{\max} - \rho_i^c) \tilde{v}_i^c \\
892 \quad \text{s.t.} \quad (\sum_{i=0}^{N_p-1} \sum_{c \in C_i} r_i^c \tilde{v}_i^c) \geq d + \mathbf{1}_{c^* < c'}, \\
893 \quad \sum_{c \in C_i} \tilde{v}_i^c = 1, \quad \forall i \in [N_p], \\
894 \quad \tilde{v}_i^c \in \{0, 1\}, \quad \forall i \in [N_p], \forall c \in C_i
\end{aligned}$$

901

We use the same trick to reverse the sign of the inequality. We will skip through the construction for the trick as it is exactly the same. Reformulating it finally gives us :

904

$$\begin{aligned}
905 \quad P_3(c') = \max_{\tilde{v}} \sum_{i=1}^{N_p} \sum_{c \in C_i} (\rho_{\max} - \rho_i^c) \tilde{v}_i^c \\
906 \quad \text{s.t.} \quad \sum_{i=0}^{N_p-1} \sum_{c \in C_i} (r_{\max} - r_i^c) \tilde{v}_i^c \leq N_p * r_{\max} - (d + \mathbf{1}_{c^* < c'}), \\
907 \quad \sum_{c \in C_i} \tilde{v}_i^c = 1, \quad \forall i \in [N_p], \\
908 \quad \tilde{v}_i^c \in \{0, 1\}, \quad \forall i \in [N_p], \forall c \in C_i
\end{aligned}$$

915

As we have explicitly specified the  $r_i^c$  values, we can see that  $r_{\max}$  is 2. The value of  $d$  is upper bounded by  $N_p$  as it is the difference in the number of votes. Thus, just as a sanity check, we can confirm that  $N_p * r_{\max} - (d + 1)$  is positive.

918 We can define  $\rho_{eff} = \rho_{max} - \rho$  and  $r_{eff} = r_{max} - r$ . Note that  $r_{eff}$  and  $\rho_{eff}$  are non-negative.  
 919 Hence we have a MCKP with positive weights and profits .  
 920

$$\begin{aligned}
 P_3(c') &= \max_{\tilde{v}} \sum_{i=1}^{N_p} \sum_{c \in C_i} (\rho_{eff})_i^c \tilde{v}_i^c \\
 \text{s.t.} \quad & \sum_{i=0}^{N_p-1} \sum_{c \in C_i} (r_{eff})_i^c \tilde{v}_i^c \leq N_p * r_{max} - (d + \mathbf{1}_{c^* < c'}), \\
 & \sum_{c \in C_i} \tilde{v}_i^c = 1, \quad \forall i \in [N_p], \\
 & \tilde{v}_i^c \in \{0, 1\}, \quad \forall i \in [N_p], \forall c \in C_i
 \end{aligned}$$

921  
 922  
 923  
 924  
 925  
 926  
 927  
 928  
 929  
 930  
 931  
 932 **Complexity.** The worst case complexity for solving the above problem is  $\mathcal{O}((N_p * r_{max} - (d +$   
 933  $\mathbf{1}_{c^* < c'})) * \sum_{i=1}^{N_p} |\mathcal{C}_i|)$  (Dudzinski & Walukiewicz, 1987). Note that  $\sum_{i=1}^{N_p} |\mathcal{C}_i| \leq 3 * N_p$ . Hence,  
 934 the worst case complexity of solving the MCKP for our use case is  $\mathcal{O}(N_p^2)$ .  $P_2(c')$  can be computed  
 935 as  $N_p * \rho_{max} - P_3(c')$ . We derive the certificate for the ensemble by solving  $P_2(c')$  for every class  
 936 and finding the minimum. Thus, we derive ensemble-level guarantees by aggregating the white-box  
 937 certificates from the base classifiers in  $\mathcal{O}(K * N_p^2)$ .  
 938

939  
 940  
 941  
 942  
 943  
 944  
 945  
 946  
 947  
 948  
 949  
 950  
 951  
 952  
 953  
 954  
 955  
 956  
 957  
 958  
 959  
 960  
 961  
 962  
 963  
 964  
 965  
 966  
 967  
 968  
 969  
 970  
 971

972 A.4 SVM SIMPLIFICATION FOR SUFFICIENTLY SMALL  $C$   
973974 **Theorem** (Restating Theorem 2). *Given a soft-margin SVM with penalty parameter  $C$ , kernel ma-  
975 trix entries  $Q_i^j$ , and dual solution  $\alpha$  to  $P_{\text{svm}}(\mathbf{y})$ , if*

976  
977 
$$C \left( \max_{i \in [n]} \sum_{j=1}^n |Q_i^j| \right) - 1 \leq 0,$$
  
978  
979

980 *then for all label assignments  $\mathbf{y} \in \{-1, 1\}^n$  we have:*  
981

982 
$$\alpha = C \cdot \mathbf{1}^n.$$

983 *That is, all dual variables are equal to  $C$ , independent of the choice of labels.*  
984985 *Proof.* We restate the dual formulation of the soft-margin SVM optimization problem for comple-  
986 ness. Given training labels  $\mathbf{y} \in \{-1, 1\}^n$  and kernel matrix entries  $Q_i^j$ , the dual problem is:  
987

988  
989 
$$P_{\text{svm}}(\mathbf{y}) = \min_{\alpha} \left( - \sum_{i=1}^n \alpha_i + \frac{1}{2} \sum_{i=1}^n \sum_{j=1}^n y_i y_j \alpha_i \alpha_j Q_i^j \right) \quad \text{s.t.} \quad 0 \leq \alpha_i \leq C \quad \forall i \in [n].$$
  
990  
991

992 The gradient of the objective  $P_{\text{svm}}(\mathbf{y})$  with respect to  $\alpha_i$  is:  
993

994  
995 
$$\frac{\partial P_{\text{svm}}(\mathbf{y})}{\partial \alpha_i} = \sum_{j=1}^n y_i y_j \alpha_j Q_i^j - 1.$$
  
996  
997

998 Over the feasible domain  $0 \leq \alpha_j \leq C \quad \forall j \in [n]$ , we can bound the derivative as:  
999

1000  
1001 
$$\frac{\partial P_{\text{svm}}(\mathbf{y})}{\partial \alpha_i} \leq C \sum_{j=1}^n |Q_i^j| - 1.$$
  
1002  
1003

1004 Now, if  $C \left( \max_{i \in [n]} \sum_{j=1}^n |Q_i^j| \right) - 1 \leq 0$ , then for every  $i \in [n]$ :  
1005

1006  
1007 
$$\frac{\partial P_{\text{svm}}(\mathbf{y})}{\partial \alpha_i} = \sum_{j=1}^n y_i y_j \alpha_j Q_i^j - 1 \leq 0.$$
  
1008  
1009

1010 This implies that  $P_{\text{svm}}(\mathbf{y})$  is monotonically decreasing in each  $\alpha_i$  over the feasible set. Hence, the  
1011 minimum is attained at the boundary:  
1012

1013 
$$\alpha_i = C \quad \forall i \in [n].$$

1014 Thus, under the stated condition on  $C$ , the solution is  $\alpha = C \cdot \mathbf{1}^n$ , *regardless of the choice of labels*  
1015  $\mathbf{y} \in \{-1, 1\}^n$ .  $\square$   
10161017 A.5 SCALABELCERT FOR THE BINARY SETTING  
10181019 Recall that for the binary setting, we wish to find the minimum number of label flips required to  
1020 change the prediction of a soft-margin SVM that uses a sufficient small  $C$  (as described in App. A.4).  
1021 Under sufficiently small  $C$ , the SVM prediction  $\hat{p}_t$  on a test sample  $t$  simplifies to  $\hat{p}_t = \sum_{i=1}^n y_i Q_{ti}$ .  
1022 We denote the perturbed training labels as  $\tilde{\mathbf{y}}$ . Then, the number of label flips required to get the  
1023 perturbed labels  $\tilde{\mathbf{y}}$  from the clean labels  $\mathbf{y}$  can be formulated as  $\frac{1}{2} \sum_{i=1}^n (1 - y_i \tilde{y}_i)$ . For the prediction  
1024  $p_t$  to change when the model is trained on the perturbed labels, the sign of the clean prediction  $\hat{p}_t$   
1025 and the tampered prediction  $p_t = \sum_{i=1}^n \tilde{y}_i Q_{ti}$  should be opposite. With this information we can  
formulate our objective as:

1026

$$1027 \quad O(\mathbf{y}) : \min_{\tilde{\mathbf{y}} \in \{-1,1\}^n} \frac{1}{2} \sum_{i=1}^n (1 - y_i \tilde{y}_i) \quad \text{s.t.} \quad \text{sign}(\hat{p}_t) \sum_{i=1}^n \tilde{y}_i Q_{ti} < 0.$$

1028

1029  
1030 We show that  $O(\mathbf{y})$  can be solved in polynomial time. The intuition being: The labels corresponding  
1031 to the largest positive contributions in  $\text{sign}(\hat{p}_t)(\sum_{i=1}^n y_i Q_t^i)$  are the most influential in determining  
1032 the prediction, so flipping these labels greedily till the prediction changes is the optimal attack from  
1033 the adversary's point of view.

1034

1035 **Proof.** We define the prediction margin to be the sum  $S = \sum_{i=1}^n \text{sign}(\hat{p}_t) y_i Q_t^i$ . Note that  $S$  is  
1036 always positive as we have included the  $\text{sign}(\hat{p}_t)$  inside the sum. The prediction for the SVM  
1037 trained on the perturbed labels  $\tilde{\mathbf{y}}$  will change when  $\tilde{S} = \sum_{i=1}^n \text{sign}(\hat{p}_t) \cdot \tilde{y}_i Q_t^i$  becomes negative.  
1038 Let  $a_i = \text{sign}(\hat{p}_t) \cdot y_i \cdot Q_{ti} \quad \forall i \in [n]$ . Thus,  $S = \sum_{i=1}^n a_i$ . Flipping a subset of the clean training  
1039 labels  $F \in 2^{[n]}$  to get the perturbed labels  $\tilde{\mathbf{y}}$  changes the  $i$ th term  $a_i$  to  $-a_i$  for  $i \in F$ , resulting in

$$1040 \quad \tilde{S} = S - 2 \sum_{i \in F} a_i.$$

1041

1042 The prediction changes when  $\tilde{S}$  is negative, i.e.,  $\sum_{i \in F} a_i > S/2$ . Hence,  $O(\mathbf{y})$  reduces to finding  
1043 the smallest subset  $F$  such that satisfies the above condition.

1044

1045 **Greedy algorithm.** Construct  $W = (a_1, \dots, a_n)$  and sort it in descending order:  $a_{(1)} \geq a_{(2)} \geq$   
1046  $\dots \geq a_{(n)}$ . Let  $P_k = \sum_{j=1}^k a_{(j)}$  be the cumulative sum of the largest  $k$  elements. We find the  
1047 smallest  $k'$  such that  $P_{k'} > S/2$  and construct the set  $F$  by including the labels corresponding to  
1048  $a_{(1)}, \dots, a_{(k')}$ . Note that  $\forall k < k' : P_k < S/2$ . We claim that  $F$  is the minimal set that we want and  
1049  $k$  is the minimum number of flips required to change the prediction of the SVM. By construction we  
1050 ensure that  $\tilde{S}$  corresponding to the label flips in  $F$  is negative. We prove that that  $F$  is the minimal  
1051 set by contradiction. Assume there exists a subset  $F' \in 2^{[n]}$  with  $|F'| = m \leq k' - 1$  such that  
1052 flipping the labels in  $F'$  results in changing the prediction of the SVM, i.e.,  $\sum_{i \in F'} a_i > S/2$ . Note  
1053 that  $\sum_{i \in F} a_i$  can be only as large as  $P_{k'-1}$ , which is the sum of the  $k' - 1$  largest elements in  $W$ . But  
1054  $P_{k'-1}$  is less than  $S/2$  as  $\forall k < k' : P_k < S/2$ . This contradicts the requirement  $\sum_{i \in F'} a_i > S/2$ .  
1055 Thus,  $F$  is the minimal subset and  $k$  is the minimum number of label flips required to change the  
1056 SVM prediction.

1057

1058 **Complexity.** Sorting  $W$  requires  $O(n \log n)$ , and scanning for  $k$  is  $O(n)$ . Hence  $O(\mathbf{y})$  is solvable  
1059 in  $O(n \log n)$  time, i.e., in polynomial time. Thus, ScaLabelCert provides a polynomial-time com-  
1060 putable exact certificate for sufficiently-wide neural networks, when their NTK is used as the SVM  
1061 kernel. The certificate for kernel regression can be derived similarly by replacing  $Q_t^i$  by  $(Q_{eff})_t^i$ ,  
1062 where  $(Q_{eff})_t^i$  can be obtained by a minor modification described in Sec. 3.2.

1063

1064

1065

1066

1067

1068

1069

1070

1071

1072

1073

1074

1075

1076

1077

1078

1079

1080  
1081

## A.6 EXACT CERTIFICATE FOR MULTICLASS WITHOUT PARTITIONING PROOF

1082  
1083  
1084  
1085  
1086  
1087  
1088  
1089  
1090  
1091  
1092  
1093  
1094  
1095  
1096

For the multi-class case, we use the one-vs-all strategy by decomposing the problem with  $K$  classes into  $K$  separate binary classification tasks. For each class  $c \in [K]$ , a binary classifier is trained to distinguish between samples of class  $c$  and samples from all other classes. Assume that  $p_c$  is the prediction score of a classifier for the learning problem corresponding to class  $c$ . Then, the class prediction  $c^*$  for a test sample is constructed by  $c^* = \arg \max_{c \in [K]} p_c$ . The labels are collected in the vector  $\mathbf{y} \in \{0, 1\}^{n \times K}$  where  $\mathbf{y}_i^c = 1$  if the class of the  $i$ th sample is  $c$  and 0 otherwise. Recall that for a test sample  $\mathbf{t}$ , the certificate  $\tilde{\rho}(\mathbf{t})$  denotes the maximum number of label flips up to which the prediction for the classifier does not change. We derive the certificate by finding for every class  $c' \in [K]$ , the minimum number of label flips required to change the prediction of the classifier to a particular class  $c'$ , and then taking the minimum over  $c'$ . The number of label flips to reach the perturbed label  $\tilde{\mathbf{y}}$  from the clean labels  $\mathbf{y}$  can be represented as  $\sum_{i=1}^N (1 - \sum_{c=1}^K y_i^c \tilde{y}_i^c)$ . For the class  $c'$  to be the predicted class, the score  $p_{c'}$  for class  $c'$  should exceed the score  $p_c$  for every other class  $c$ . Using a soft-margin kernel SVM with a sufficiently small  $C$  as our base model, the score  $p_c$  can be written as  $p_c = \sum_{i=1}^N y_i^c Q_{ti}$ . With this information, the minimum number of label flips required to change the prediction of the model to a particular class  $c'$  can be formulated as:

1097  
1098  
1099  
1100  
1101  
1102  
1103  
1104

$$O_1(c') : \min_{\tilde{\mathbf{y}}} \sum_{i \in [N]} \left( 1 - \sum_{c \in [K]} y_i^c \tilde{y}_i^c \right) \quad \text{s.t.} \quad \sum_{i \in [n]} \tilde{y}_i^{c'} Q_t^i > \sum_{i \in [N]} \tilde{y}_i^c Q_t^i \quad \forall c \neq c',$$

$$\forall i \in [n], c \in [K] : \sum_{c \in [K]} \tilde{y}_i^c = 1, \tilde{y}_i^c \in \{0, 1\}.$$
(7)

1105  
1106  
1107  
1108  
1109

The certificate  $\tilde{\rho}(\mathbf{t})$  can be calculated as:  $\tilde{\rho}(\mathbf{t}) = \min_{c' \in [K] \setminus \{c^*\}} O_1(c') - 1$ .  $O_1(c')$  is a Integer Linear Program(ILP) with  $n \times K$  binary variables. Hence, the complexity for solving  $O_1(c')$  the problem is  $\mathcal{O}(2^{n \times K})$ . Consequently, the complexity for deriving  $\tilde{\rho}(\mathbf{t})$ , which is calculated by taking the minimum over  $O_1(c')$ , is  $\mathcal{O}(K \times 2^{n \times K})$ . This prompts us to solve a simpler alternative  $O_2(c')$  instead, that relaxes the constraint in  $O_1(c')$  requiring  $c'$  to be the predicted class:

1110  
1111  
1112  
1113  
1114  
1115  
1116  
1117

$$O_2(c') : \min_{\tilde{\mathbf{y}}} \sum_{i \in [N]} \left( 1 - \sum_{c \in [K]} y_i^c \tilde{y}_i^c \right) \quad \text{s.t.} \quad \sum_{i \in [n]} \tilde{y}_i^{c'} Q_t^i > \sum_{i \in [N]} \tilde{y}_i^{c^*} Q_t^i,$$

$$\forall i \in [n], c \in [K] : \sum_{c \in [K]} \tilde{y}_i^c = 1, \tilde{y}_i^c \in \{0, 1\}.$$
(8)

1118  
1119  
1120  
1121

$O_2(c')$  calculates the minimum number of label flips needed to make the prediction score  $p_{c'}$  for class  $c'$  exceed the prediction score  $p_{c^*}$  for the original predicted class  $c^*$ . Notably, this relaxation is similar to the relaxation of  $P_1(c')$  to  $P_2(c')$  in the context of computing the certificate for the ensemble. Despite the relaxation, we show that the minimum over  $O_1(c')$  is preserved, i.e.:

1122  
1123  
1124

$$\min_{c' \in [K] \setminus \{c^*\}} O_1(c') = \min_{c' \in [K] \setminus \{c^*\}} O_2(c')$$

1125  
1126  
1127  
1128  
1129  
1130  
1131  
1132  
1133

The intuition being — while trying to make  $c'$  surpass  $c^*$ , if another class  $c''$  becomes the predicted class, then changing the classifier prediction to  $c''$  should be easier compared to  $c'$ . As the design of the relaxation and the intuition are similar to the ensemble case, the proof strategy for this result is exactly the same as Theorem 1. The only difference would be that the notation **majVote**( $\tilde{\mathbf{V}}$ ), that finds the majority class for a vote configuration  $\tilde{\mathbf{V}}$  will be replaced by the **majScore** notation that predicts the class when the model is trained on the perturbed labels  $\tilde{\mathbf{y}}$ , i.e.  $\text{majScore}(\tilde{\mathbf{y}}) = \arg \max_{c \in [K]} \sum_{i \in [n]} \tilde{y}_i^c Q_t^i$ . Hence, we direct the reader to the proof for Theorem 1 provided in App. A.2. With the above result, we can derive the certificate  $\tilde{\rho}(\mathbf{t})$  as:  $\tilde{\rho}(\mathbf{t}) = \min_{c' \in [K] \setminus \{c^*\}} O_2(c')$  — 1

1134 **Solving  $O_2(c')$ .** We focus our attention on solving  $O_2(c')$ . Recall that  $O_2(c')$  denotes the minimum  
 1135 number of label flips needed to make the prediction score  $p_{c'}$  for class  $c'$  exceed the prediction score  
 1136  $p_{c^*}$  for the original predicted class  $c^*$ .  
 1137

1138 We denote the training samples that were labeled  $c^*$  originally as  $P_{\text{maj}}$  and samples that were labeled  
 1139  $c'$  originally as  $P_{\text{target}}$ .  $P_{\text{rest}}$  denote the set of remaining samples  
 1140

$$1141 P_{\text{maj}} = \{i \in [N] \mid y_i^{c^*} = 1\}, \quad P_{\text{target}} = \{i \in [N_p] \mid y_i^{c'} = 1\}, \quad P_{\text{rest}} = [n] \setminus P_{\text{maj}} \cup P_{\text{target}}$$

1142 Let  $d$  be the original difference between score for  $c'$  and  $c^*$ :  $d = \sum_i (y_i^{c^*} - y_i^{c'}) Q_{ti}$ . We define  $r_i^c$   
 1143 to be the **reduction** caused by flipping label of the  $i$ th sample to class  $c$  in the difference between  
 1144 score for  $c'$  and  $c^*$ . For the score  $p_{c'}$  exceed the score  $p_{c^*}$ , the total reduction caused by the label  
 1145 flipping attack should exceed  $d$ . Lets see what these values will be for different  $i$  and  $c$ . **For samples**  
 1146 **in  $P_{\text{maj}}$ .** For samples that were originally labeled  $c^*$ , if the label is flipped to  $c'$ , reduction will be  
 1147  $2 * Q_{ti}$ . If the label is flipped from  $c^*$  to any other class, the reduction is only by  $Q_{ti}$  as it affects  
 1148 the score only for  $c^*$ . If  $Q_{ti}$  is positive, flipping the label to  $c'$  will cause the maximum reduction  
 1149 possible by flipping the  $i$ th label. Hence, an optimal attack will flip the  $i$ th label to  $c'$  (if it chooses  
 1150 to flip the label). If  $Q_{ti}$  is negative, an optimal attack will not flip the label for the  $i$ th sample as it  
 1151 will further increase the gap between  $c'$  and  $c^*$ .  
 1152

$$1153 \forall i \in P_{\text{maj}}, c \in [K], \quad r_i^c = \begin{cases} 2 * Q_{ti} & \text{if } c = c' \\ 0 & \text{else if } c = c^* \\ Q_{ti} & \text{else} \end{cases}$$

1156 **For samples in  $P_{\text{target}}$ .** Following a similar line of argument as above, we can safely say that  
 1157  $\forall i \in P_{\text{target}}$ , if  $Q_{ti} < 0$ , an optimal attack will flip the label for sample  $i$  to  $c^*$  (if it chooses to flip the  
 1158 label). If  $Q_{ti}$  is positive, an optimal attack will not flip the label for the  $i$ th sample as it will further  
 1159 increase the gap between  $c'$  and  $c^*$ .  
 1160

$$1161 \forall i \in P_{\text{target}}, c \in [K], \quad r_i^c = \begin{cases} -2 * Q_{ti} & \text{if } c = c^* \\ 0 & \text{else if } c = c' \\ -Q_{ti} & \text{else} \end{cases}$$

1165 **For samples in  $P_{\text{rest}}$ .** For samples with the true label other than  $c'$  or  $c^*$ , if  $Q_{ti} > 0$ , an optimal  
 1166 attack will flip the  $i$ th label to  $c'$ . If  $Q_{ti}$  is negative, the optimal attack will flip the  $i$ th label to  $c^*$ , if  
 1167 it chooses to flip the label.  
 1168

$$1169 \forall i \in P_{\text{rest}}, c \in C_i, \quad r_i^c = \begin{cases} Q_{ti} & \text{if } c = c' \\ -Q_{ti} & \text{if } c = c^* \\ 0 & \text{else} \end{cases}$$

1173 With this, we can define  $r(i)$  as the reduction in the difference between scores for  $c'$  and  $c^*$  in the  
 1174 optimal attack, if the attacker chooses to flip the  $i$ th label:  $\forall i \in [N], r(i) = \max_{c \in [K]} r_i^c$ . Note  
 1175 that if  $r_i$  is 0, the  $i$ th label will not be flipped. Hence we define the set of candidates for flipping the  
 1176 labels as  $E_f$ :  $E_f = \{i \in [N] \mid r(i) > 0\}$   
 1177

We employ a greedy strategy similar to the one used in the computation of the certificate for the  
 1178 binary case (App. A.5). We first sort the candidate flipping labels  $E_f$  based on their  $r(i)$  values in  
 1179 the descending order, i.e.,  $r_{(1)} \geq r_{(2)} \geq \dots$ . Let  $P_k = \sum_{j=1}^k r_{(j)}$  be the cumulative sum of the  
 1180 largest  $k$  elements. We find the smallest  $k'$  such that  $P_{k'} > d$  and construct  $G_{k'}$  by including the  
 1181 indices corresponding to the  $k'$  largest  $r(i)$  values. We claim that  $k'$  is the minimum number of label  
 1182 flips required to make the score for  $c'$  exceed  $c^*$  and  $G_{k'}$  is the minimal set of the labels that need to  
 1183 be flipped to make it happen. The greedy algorithm is illustrated in Algorithm 1.  
 1184

We prove optimality by contradiction. Recall that  $G_k = \{(1), \dots, (k)\}$  is the greedy choice of  $k$   
 1185 largest  $r(i)$  and  $P_k = \sum_{j=1}^k r_{(j)}$ . Suppose there exists a set  $F \subseteq E_f$  with  $|F| = m \leq k' - 1$   
 1186 such that flipping labels in  $F$  achieves the objective, i.e.,  $\sum_{i \in F} r(i) > d$ . But  $G_m$  consists of the  $m$   
 1187 largest  $r(i)$ , so  $\sum_{i \in F} r(i) \leq \sum_{i \in G_m} r(i) = P_m \leq P_{k'-1} \leq d$ , a contradiction.  
 1188

1188 **Algorithm 1** Greedy Certificate Computation1189 **Input:** Score gap  $d$ , reductions  $r(1), \dots, r(n)$ 1190 **Output:** Minimum number of flips  $k$ 

```

1191   1: total_red  $\leftarrow 0$ 
1192   2: sorted  $\leftarrow \text{sort}(r, \text{descending})$ 
1193   3:  $i \leftarrow 0$ 
1194   4: while total_red  $< d$  do
1195     5:   total_red  $\leftarrow$  total_red + sorted[ $i$ ]
1196     6:    $i \leftarrow i + 1$ 
1197   7: end while
1198   8: return  $i$ 
```

1199

1200

1201 **Complexity.** Sorting based on the reduction values takes  $\mathcal{O}(n \log n)$ , and scanning for the minimal  
 1202  $k'$  takes  $\mathcal{O}(n)$ . Solving  $O_2(c')$  for all  $c' \in [K] \setminus c^*$  can be done in  $\mathcal{O}(Kn \log n)$ , resulting in a  
 1203 polynomial-time **exact** certificate for test sample  $\mathbf{t}$ :  $\tilde{\rho}(\mathbf{t}) = \min_{c' \neq c^*} O_2(c') - 1$ .

1204

1205

1206

1207

1208

1209

1210

1211

1212

1213

1214

1215

1216

1217

1218

1219

1220

1221

1222

1223

1224

1225

1226

1227

1228

1229

1230

1231

1232

1233

1234

1235

1236

1237

1238

1239

1240

1241

1242 A.7 EXTRACTING WHITE-BOX KNOWLEDGE FOR THE MULTI-CLASS SETTING  
1243

1244 Recollect that EnsembleCert utilizes the white-box knowledge  $\rho_i^c$  for all base classifiers  $i \in [N_p]$   
1245 and all classes  $c \in [K]$  where  $\rho_i^c$  denotes the minimum number of flips required to change the  
1246 prediction of the  $i$ th base classifier to  $c$ . For each base classifier, using a soft-margin kernel SVM  
1247 with a sufficiently small  $C$  as our base model, we formulate the problem of finding the minimum  
1248 number flips required to change the prediction of the classifier to  $c'$  is formulated as:

$$1249 \quad 1250 \quad 1251 \quad O_1(c') : \min_{\tilde{\mathbf{y}}} \sum_{i \in [N]} \left( 1 - \sum_{c \in [K]} y_i^c \tilde{y}_i^c \right) \quad \text{s.t.} \quad \sum_{i \in [n]} \tilde{y}_i^{c'} Q_t^i > \sum_{i \in [N]} \tilde{y}_i^c Q_t^i \quad \forall c \neq c', \\ 1252 \quad 1253 \quad 1254 \quad \forall i \in [n], c \in [K] : \sum_{c \in [K]} \tilde{y}_i^c = 1, \tilde{y}_i^c \in \{0, 1\}. \\ 1255 \quad 1256$$
(9)

1257 The above problem is an ILP with  $n \times K$  binary variables, resulting in a computational complexity  
1258 of  $\mathcal{O}(2^{nK})$ . For each base classifier, we need to solve this problem for all classes. Consider  
1259 an ensemble with  $N_p$  base classifiers. We would need to solve  $N_p \times K$  ILPs with the computational  
1260 complexity of  $O_1(c')$ , making the problem intractable. Hence, instead of solving the problem  
1261  $O_1(c')$  exactly, we bound the problem efficiently, and show that our bounds are sufficiently tight on  
1262 empirical evaluation.

1263 A.7.1 LOWER BOUND  
1264

1265 For the purpose of computing the exact certificate for the multiclass case in the no partition case, we  
1266 formulated an alternate problem  $O_2(c')$  (Eq. (8)), a relaxed version of  $O_1(c')$  which only requires  
1267 the score  $p_{c'}$  for class  $c'$  to exceed the score  $p_{c^*}$  for class  $c^*$ . We showed in App. A.6 that  $O_2(c')$  can  
1268 be solved in polynomial time. As the constraint set of  $O_2(c')$  is a subset of  $O_1(c')$ , the solution for  
1269  $O_2(c')$  will always be less than or equal to  $O_1(c')$ . Hence,  $O_2(c')$  represents a valid lower bound on  
1270  $O_1(c')$ , that is polynomial-time calculable. Notably,  $O_2(c')$  is also a certificate by definition, as it is  
1271 a lower bound on the certified radius.

1272 A.7.2 UPPER BOUND  
1273

1274 To compute a valid upper bound on  $O_1(c')$ , finding an instance of perturbed labels  $\tilde{\mathbf{y}}$  that satisfies  
1275 the constraints of  $O_1(c')$ , i.e.,  $\text{majScore}(\tilde{\mathbf{y}}) = c'$ , is sufficient. The number of label flips needed to  
1276 reach any such  $\tilde{\mathbf{y}}$  from the clean labels  $\mathbf{y}$  represents a valid upper bound on  $O_1(c')$ . To compute  
1277 this upper bound efficiently, we adopt a greedy strategy that iteratively flips training labels to reach a  
1278 feasible solution of Eq. (1). At the beginning of each iteration, we compute the current majority class  
1279  $c^* = \arg \max_c S_c$ , where  $S_c = \sum_{i=1}^n \tilde{y}_i^c Q_t^i$  is the score of class  $c$ . Note that  $c^*$  may change after  
1280 each label flip, and our method accounts for this by re-evaluating  $c^*$  and all per-sample damages  
1281  $d_i$  after every label flip. Let  $S^{(2)} = \max_{c \in [K] \setminus c^*} S_c$  denote the score of the runner-up class. For  
1282 each sample  $i$ , we define the *per-sample damage*  $d_i$  as the maximum possible reduction in the gap  
1283 between  $c'$  and the majority class achievable by flipping  $i$ :

$$1284 \quad 1285 \quad d_i = \begin{cases} \min(2Q_t^i, Q_t^i + S_{c^*} - S^{(2)}), & \text{if } \tilde{y}_i^{c^*} = 1 \text{ and } Q_t^i > 0, \\ 1286 \quad 1287 \quad \min(2|Q_t^i|, |Q_t^i| + S_{c^*} - S^{(2)}), & \text{else if } \tilde{y}_i^{c'} = 1 \text{ and } Q_t^i < 0, \\ 1288 \quad 1289 \quad Q_t^i, & \text{if } \tilde{y}_i^{c^*} = 0, \tilde{y}_i^{c'} = 0, \text{ and } Q_t^i > 0, \\ 1290 \quad 1291 \quad 0, & \text{otherwise.} \end{cases}$$

1292 Intuitively,  $d_i$  captures the maximal contribution that flipping sample  $i$  can make toward satisfying  
1293 the class-change constraint of Eq. (1).

1294 Cases explained  
1295

1296 1. **Case 1** ( $\tilde{y}_i^{c^*} = 1, Q_t^i > 0$ ): Flipping a positively contributing  $c^*$ -labeled sample to  $c'$  both  
 1297 reduces  $S_{c^*}$  and increases  $S_{c'}$ , leading to a decrease of  $2Q_t^i$ . The possibility that the runner-  
 1298 up class becomes the majority is considered by the term  $Q_t^i + S_{c^*} - S^{(2)}$ , which accounts  
 1299 for the score gap to the second-highest class.  
 1300 2. **Case 2** ( $\tilde{y}_i^{c'} = 1, Q_t^i < 0$ ): Flipping a negatively contributing  $c'$ -labeled sample to  $c'$  helps  
 1301 both by increasing  $S_{c'}$  and decreasing  $S_{c^*}$ , giving a decrease of  $2|Q_t^i|$ . The possibility of  
 1302 runner-up class becoming the majority class is handled as above.  
 1303 3. **Case 3 (neutral sample,  $Q_t^i > 0$ )**: Flipping such a sample to  $c'$  only increases  $S_{c'}$ , so the  
 1304 reduction in the gap is exactly  $Q_t^i$ .

1305  
 1306 In each iteration, we select  $i^* = \arg \max_i d_i$ , flip the corresponding label to  $c'$  or  $c^*$ , re-evaluate  
 1307 the majority class, and repeat this process until  $c'$  becomes the majority class. Hence, by design,  
 1308 the greedy algorithm results in a feasible  $\tilde{\mathbf{y}}$  satisfying Eq. (1), and the number of flips performed  
 1309 constitutes a valid upper bound on  $O_1(c')$ . Our greedy approach is illustrated in Algorithm 2.

1310 **Complexity.** We choose the label to flip by calculating the possible reduction each label flip can  
 1311 cause in the gap between  $c^*$  and  $c'$ , and choosing the one that causes the maximum reduction. This  
 1312 involves scanning the dataset at every iteration. Hence the worst case complexity in computing the  
 1313 upper bound for  $O_1(c')$  is  $\mathcal{O}(n^2)$ .  
 1314

---

1315 **Algorithm 2** Greedy Upper Bound Computation for  $O_1(c')$

---

1316 1: **Input:** Clean labels  $\mathbf{y}$ , kernel entries corresponding to the  $i$ th training sample and test sample  
 1317  $t: Q_t^i \forall i \in [N]$ , target class  $c'$   
 1318 2: **Output:** Upper bound on  $O_1(c')$  (number of label flips)  
 1319 3: Initialize  $\tilde{\mathbf{y}} \leftarrow \mathbf{y}$   
 1320 4: Compute  $S_c = \sum_{i=1}^N \tilde{y}_i^c Q_t^i$  for all  $c \in [K]$   
 1321 5:  $c^* \leftarrow \arg \max_c S_c$   
 1322 6: **while**  $c^* \neq c'$  **do**  
 1323   7:    $S^{(2)} \leftarrow \max_{c \neq c^*} S_c$   
 1324   8:   **for**  $i = 1$  to  $N$  **do**  
 1325     9:     **if**  $\tilde{y}_i^{c^*} = 1$  and  $Q_t^i > 0$  **then**  
 1326       10:      $d_i \leftarrow \min(2Q_t^i, Q_t^i + S_{c^*} - S^{(2)})$   
 1327     **else if**  $\tilde{y}_i^{c'} = 1$  and  $Q_t^i < 0$  **then**  
 1328       12:      $d_i \leftarrow \min(2|Q_t^i|, |Q_t^i| + S_{c^*} - S^{(2)})$   
 1329     **else if**  $\tilde{y}_i^{c^*} = 0$  and  $\tilde{y}_i^{c'} = 0$  and  $Q_t^i > 0$  **then**  
 1330       14:      $d_i \leftarrow Q_t^i$   
 1331     **else**  
 1332       16:      $d_i \leftarrow 0$   
 1333     **end if**  
 1334   **end for**  
 1335   19:    $i^* \leftarrow \arg \max_i d_i$   
 1336   20:   **if**  $\tilde{y}_{i^*}^{c'} = 1$  **then**  
 1337     21:      $\tilde{y}_{i^*}^{c^*} \leftarrow 1$   
 1338     **else**  
 1339       23:      $\tilde{y}_{i^*}^{c'} \leftarrow 1$   
 1340     **end if**  
 1341   25:   Update  $S_c = \sum_{i=1}^N \tilde{y}_i^c Q_t^i$  for all  $c \in [K]$   
 1342   26:    $c^* \leftarrow \arg \max_c S_c$   
 1343 27: **end while**  
 1344 28: **return** Number of flips applied to reach  $\tilde{\mathbf{y}}$

---

1345  
 1346  
 1347  
 1348  
 1349

1350 **B DETAILS OF RANDOMIZED SMOOTHING INTEGRATION**  
13511352 **B.1 SMOOTHED LINEAR CLASSIFIER AS THE BASE MODEL**  
1353

1354 In addition to ScaLabelcert for sufficiently wide networks, we use the method from Rosenfeld et al.  
1355 (2020) for certification of base classifiers. Their approach uses a smoothed linear classifier as the  
1356 base classifier. The smoothing process involves independently flipping each label with probability  $q$   
1357 and assigning a flipped label uniformly at random among the remaining  $K - 1$  classes. To certify  
1358 robustness, the method bounds the probability that this randomized classifier switches its prediction  
1359 from one class to another.

1360 **B.2 PREDICTION BY THE SMOOTHED CLASSIFIER**  
1361

1362 The method by Rosenfeld et al. (2020) computes, for each pair of classes  $(c, c')$ , a Chernoff bound  
1363  $p_{c,c'}(q)$  that gives an upper-bound on the probability that the randomized classifier switches its  
1364 predicted class from  $c$  to  $c'$  under the randomized label flips.

1365 For each class  $c$ , the method evaluates

$$\max_{c' \neq c} p_{c,c'}(q)$$

1366 and defines the predicted class as  
1367

$$c^* = \arg \min_{c \in [K]} \max_{c' \neq c} p_{c,c'}(q),$$

1372 **B.3 COMPUTING THE CERTIFICATE**  
1373

1374 The certified radius  $r$  is obtained by plugging the worst-case probability bound  $\max_{c' \neq c^*} p_{c^*,c'}(q)$   
1375 into the robustness guarantee from a result in Rosenfeld et al. (2020), giving

$$r \leq \frac{\log(4p(1-p))}{2(1-2q)\log(\frac{q}{1-q})},$$

1376 where  $p = \max_{c' \neq c^*} p_{c^*,c'}(q)$ . This bound guarantees that if at most  $r$  labels were flipped by the  
1377 adversary, the smoothed classifier would still predict  $c^*$ .  
1378

1382 **B.4 ADAPTATION FOR OUR USE CASE**  
1383

1384 We follow the same prediction rule to obtain  $c^*$ . However, instead of computing the radius that  
1385 certifies that the prediction will not change to *any* other class, we focus on certifying robustness  
1386 against a specific target class  $c'$ . This is because our objective is to compute the minimum number  
1387 of label flips required to change the prediction of a base classifier to *every* class. This white-  
1388 box information is then used by EnsembleCert to construct a white-box infused certificate for the  
1389 ensemble.

1390 Concretely, we use the pairwise Chernoff bound  $p_{c^*,c'}(q)$  and compute  
1391

$$r_{c'} \leq \frac{\log(4p_{c^*,c'}(1-p_{c^*,c'}))}{2(1-2q)\log(\frac{q}{1-q})},$$

1392 which gives the number of label flips required to change the prediction specifically from  $c^*$  to  $c'$ .  
1393

## C ADDITIONAL PLOTS

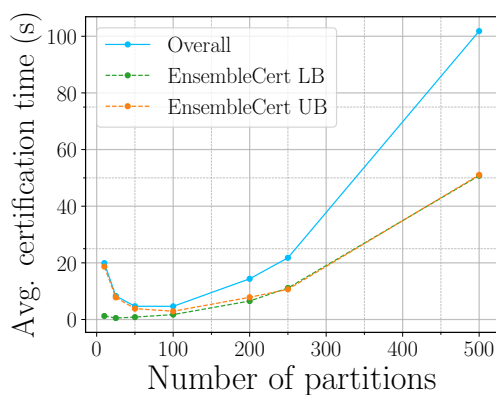
## C.1 FURTHER IMPLEMENTATION DETAILS AND CERTIFICATION RUNTIME

**Hardware.** All the experiments were done on an internal cluster. We used GPUs solely for the NTK kernel computation, which was done using the Google neural-tangents library (Novak et al., 2020). As the kernel computation is not the main focus of our work, we refer interested readers to (Novak et al., 2020) for details on latency and memory requirements. All the following steps for certificate derivation were executed on CPUs.

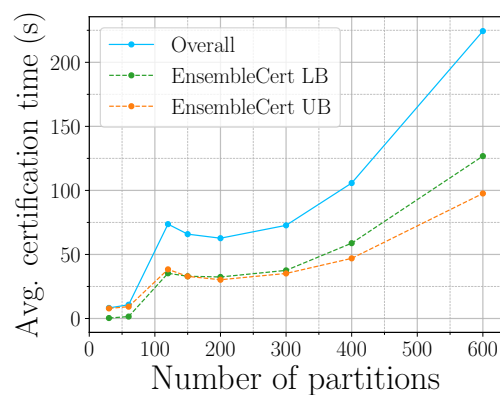
**Certificate derivation.** We process the test data in parallel batches of 100 samples. Recall that for each test sample, EnsembleCert first computes  $\rho_i^c$  for every base classifier  $i \in [N_p]$  and class  $c \in [K]$  using ScaLabelCert, which provides both upper and lower bounds. This requires computing  $N_p \times K$  entries before passing this information to EnsembleCert for aggregation. In the current implementation, white-box information is computed sequentially by iterating over the partitions and classes. However, these computations are inherently parallelizable across both partitions and classes because the certificates are independent. In particular, the lower bound calculation for each  $\rho_i^c$  (App. A.7.1) can be fully vectorized, whereas the upper bound calculation (App. A.7.2) must be performed independently for each sample. The aggregation step, which combines white-box information to derive the ensemble-level certificate, is also executed independently per sample. This step involves solving a Multiple-Choice Knapsack Problem (MCKP) for each test sample, which to the best of our knowledge, cannot be vectorized efficiently.

**Average Certification Time per Sample.** As discussed, both EnsembleCert and ScaLabelCert yield polynomial-time computable certificates. Since lower bound computations are vectorized within each batch, per-sample latency cannot be measured directly. Instead, we report average amortized time, which refers to the total time taken to certify a batch divided by the number of samples in that batch, providing a fair per-sample estimate. We present this average amortized certification time per sample for EnsembleCert in Fig. 4. Latencies presented in the figure above also include the training and prediction latencies, which are negligible owing to the simplification under small  $C$  for kernel SVM and the closed form solution for kernel Regression. The total certification time per sample is the sum of the latencies for the upper and lower bound computations. Importantly, the upper bound latency is not amortized since the computation is performed sequentially per sample.

For small  $N_p$ , the number of samples per partition is high, which leads to a noticeable gap between the latencies of upper and lower bound computations. This is because (i) the lower bound computation is linear in the number of samples whereas the upper bound computation is quadratic and (ii) lower bounds computation is vectorized whereas upper bound computation is done independently. As  $N_p$  increases, white-box aggregation latency for both computations becomes dominant due to the quadratic complexity of MCKP in  $N_p$ , thereby narrowing the gap between the upper and lower bound curves. For CIFAR-10, the average (amortized) certification time per sample goes from as low as 5 seconds for  $N_p = 50$  to as high as under 2 minutes for  $N_p = 500$ . For MNIST, the average amortized latency varies from 8 sec to a max of around 4 min.



(a) CIFAR-10 Kernel SVM



(b) MNIST Kernel SVM

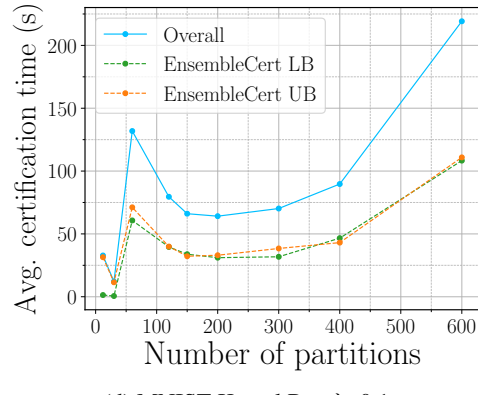
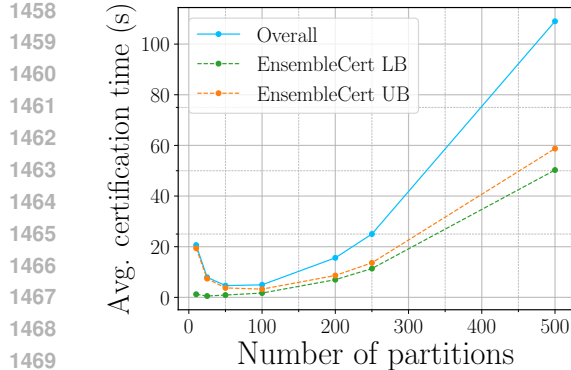
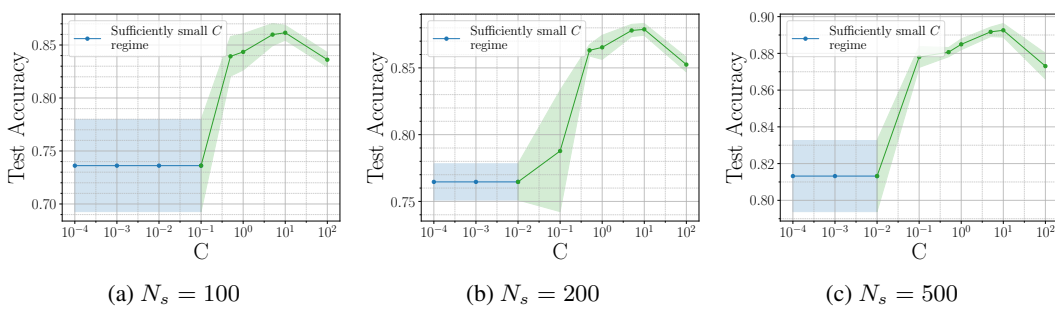


Figure 4: Figures (a) and (b) show the average latency per sample for kernel SVM on CIFAR-10 and MNIST, respectively. Figures (c) and (d) present the corresponding results for kernel regression. We report results for a single value of  $\lambda$  for each dataset, as the trends are consistent across different  $\lambda$  values and do not provide any additional qualitative insight.

**Choosing  $N_p$ .** Sec. 4 discussed the invariance of robustness to partitioning observed for EnsembleCert with kernel SVMs, and the robustness decay observed with sufficiently regularized kernel regression. This raises questions about the practical utility of using heavy partitioning. Moreover, the experiments in Fig. 4 show that larger ensembles are computationally more expensive to certify using EnsembleCert. When robust base classifiers are employed, it becomes evident that using a low to medium number of partitions offers the best trade-off between achieving high certified robustness and minimizing computational costs.

## C.2 ROBUSTNESS-ACCURACY TRADEOFF FOR SMALL $C$

Recall that the key to obtaining polynomial-time computable certificates by ScaLabelCert for infinitely-wide networks trained on the hinge loss is choosing a sufficiently small value of  $C$ . Hence, this introduces a robustness-accuracy tradeoff as we are constrained to choose  $C$  that is sufficiently small to achieve the polynomial-time certificate. To study this tradeoff, we perform 5-fold cross-validation for different values of  $C$ . For every number of partitions, the accuracy initially remains constant up to a certain threshold, indicating the range of sufficiently small  $C$ , as SVM performance does not depend on  $C$  in this regime. The results for CIFAR-10 are shown in Fig. 6. In addition to studying the tradeoff on an ensemble level, we conduct experiments to study the performance trade-off induced by "sufficiently small  $C$ " for stand-alone classifiers as a function of the training set size  $N_s$ . For each value of  $N_s$ , we sub-sample the training set for 5 different random seeds while keeping class balance. The models trained on the sub-sampled training data are evaluated on the entire test dataset. The results can be seen in Fig. 5. It is evident from these experiments that performance remains competitive in the small  $C$  regime. We do not evaluate on MNIST, as for our chosen kernel and RotNet preprocessing, the threshold for sufficiently small  $C$  is significantly larger (order of  $10^2$ ).



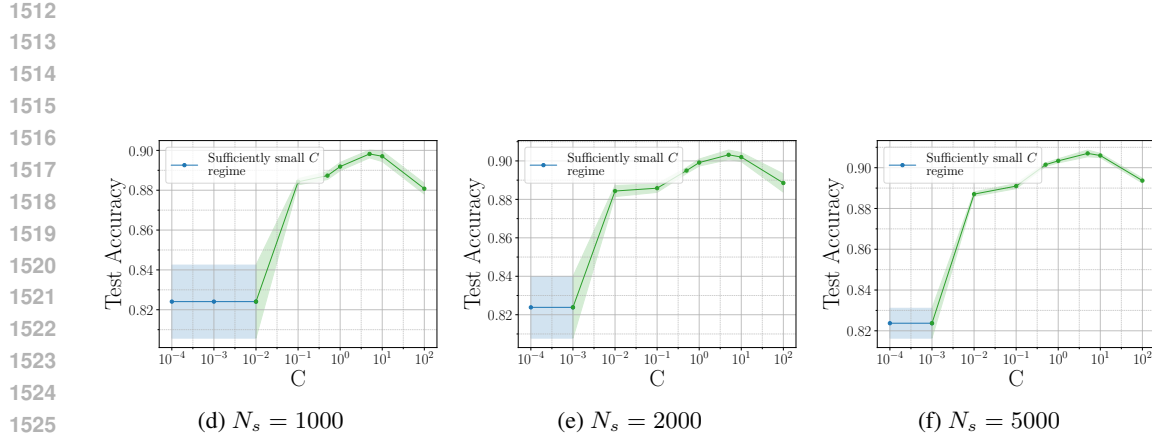


Figure 5: Performance of an infinitely-wide neural network with a single trained on hinge loss across different values of  $C$  and the cardinality of the training dataset  $N_s$ . For each value of  $N_s$ , we subsample the training set for 5 different random seeds. The accuracy for each value of  $N_s$  initially remains constant up to a certain threshold for  $C$ , indicating the range of sufficiently small  $C$ , as the SVM performance does not depend on  $C$  in this regime. Shading around the central line indicates the standard deviation. In each plot, the region of sufficiently small  $C$  is colored blue for distinction. For each plot, the accuracy initially remains constant up to a certain threshold, indicating the range of sufficiently small  $C$ , as SVM performance does not depend on  $C$  in this regime.

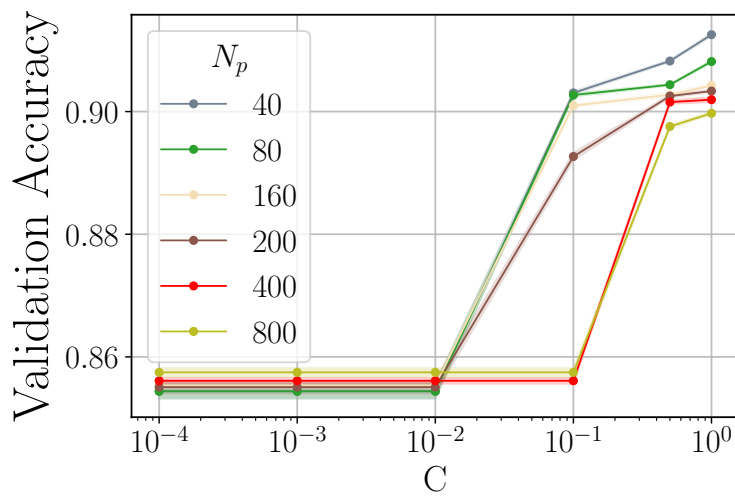
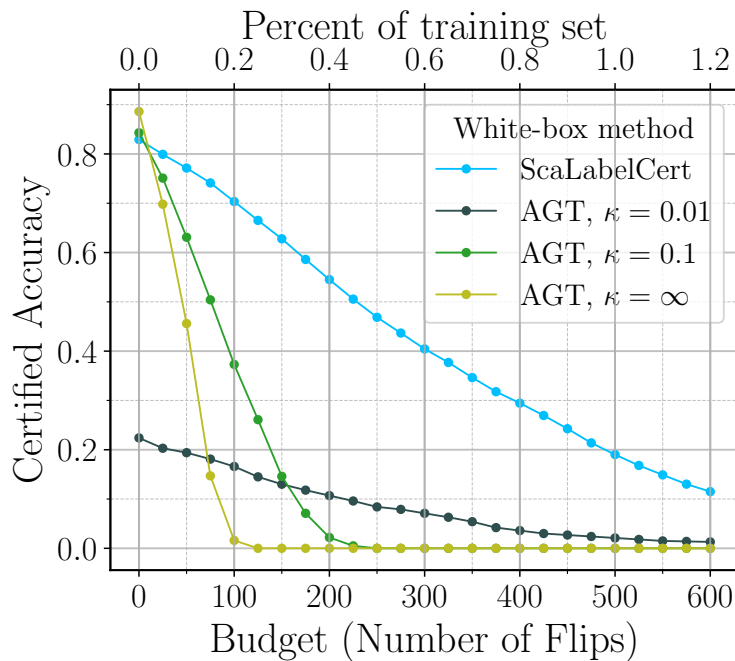


Figure 6: Robustness-accuracy trade-off introduced by sufficiently small  $C$ . While Fig. 5 studies empirical performance of stand-alone models, the impact of small  $C$  on the empirical performance of the ensemble is studies here.

1566 **C.3 COMPARISON OF SCALABELCERT WITH THE GRADIENT-BASED BOUNDING**  
 1567 **CERTIFICATE (SOSNIN ET AL., 2024)**

1569 We compare the performance of ScaLabelCert with the gradient-based parameter bounding method  
 1570 proposed by Sosnin et al. (2024) on CIFAR-10. The gradient-based approach uses convex relaxations to over-approximate all possible parameter updates under a given poisoning threat model.  
 1571 The parameter bounds are then propagated to bound the logits for individual classes. The robustness  
 1572 of the prediction for a particular sample can then be certified by checking if the lower bound on the  
 1573 output logit for the predicted class is greater than the upper bounds of all other classes given the  
 1574 perturbation budget. If this condition is satisfied, the prediction is certifiably robust under the given  
 1575 budget. To evaluate this method, we add a linear layer on top of the CIFAR-10 features extracted via  
 1576 SimCLR. We train the network for 2 epochs and keep other parameters consistent with the codebase  
 1577 for Sosnin et al. (2024). For ScaLabelCert, the same SimCLR features are input to an infinitely wide  
 1578 fully-connected network with a single hidden layer and no non-linear activation, as described in  
 1579 Sec. 4. Although the models are not identical, the architectures are structurally aligned as both mod-  
 1580 els rely on fully connected layers without activations, making the comparison meaningful. As shown  
 1581 in App. C.3, ScaLabelCert consistently outperforms the gradient-based method. This improvement  
 1582 highlights the importance of exact certification: while the gradient-based approach is inherently lim-  
 1583 ited by the looseness of its over-approximations, ScaLabelCert provides tight guarantees, resulting  
 1584 in stronger certified robustness.



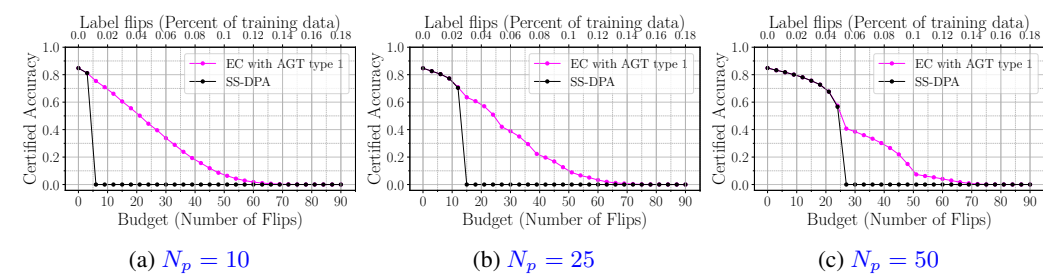
1608 **Figure 7: Comparison of ScaLabelCert and gradient-based parameter bounding method. The pa-  
 1609 rameter  $\kappa$  represents the gradient clipping parameter. ScaLabelCert significantly outperforms the  
 1610 gradient-based method for all values of  $\kappa$ .**

1620 C.4 ENSEMBLECERT WITH FINITE-WIDTH NETWORKS AS BASE CLASSIFIERS  
1621

1622 The certificates derived by ScaLabelCert are asymptotically exact and deterministic for neural  
1623 networks as the width of the network goes to infinity. Hence, ScaLabelCert is best suited for certifying  
1624 infinite-width neural networks. To demonstrate that EnsembleCert can provide deterministic certi-  
1625 ficates even when finite-width networks are used as base classifiers, we instantiate EnsembleCert  
1626 with a fully connected linear classifier as the base model and utilize the gradient-based parameter  
1627 bounding method by Sosnin et al. (2024), introduced in the previous section, to certify the base  
1628 classifiers. The gradient-based method certifies, for a given sample, whether the model’s prediction  
1629 remains unchanged when at most  $r$  training labels are flipped. However, this guarantee does not  
1630 directly match the white-box quantity required by EnsembleCert, which is the minimum number of  
1631 label flips needed to change the prediction to a *particular* class. In what follows, we explain how  
1632 this gradient-based certificate can be incorporated into EnsembleCert..  
1633

1633 **Certificate alignment.** For any certificate that verifies whether a model’s prediction remains robust  
1634 under a fixed perturbation budget of  $r$  label flips, one can obtain a certificate for the *minimum* number  
1635 of label flips needed to change the prediction to *some* class by applying the fixed-budget certificate  
1636 incrementally—starting at  $r = 0$  and increasing  $r$  until the certificate first indicates non-robustness.  
1637 Note that EnsembleCert requires white-box information quantifying the minimum number of label  
1638 flips needed to change the prediction of a base classifier to a *specific* target class. The certificate that  
1639 computes the minimum flips needed to change the prediction to *some* class then serves as a valid  
1640 lower bound on  $\rho_i^c$ , the minimum number of label flips required to force the  $i$ -th base classifier to  
1641 predict a particular class  $c$ . This relationship enables us to incorporate the gradient-based certificate  
1642 into EnsembleCert.

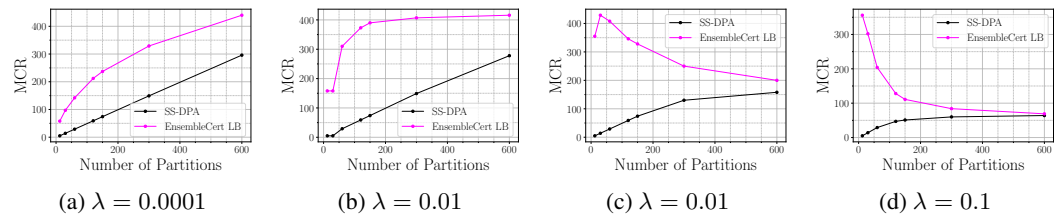
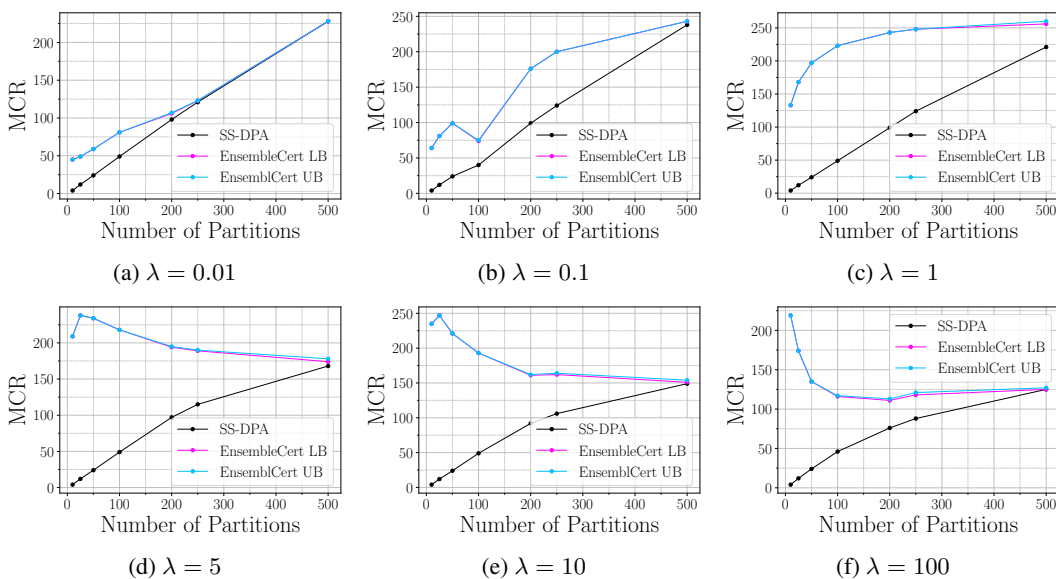
1643 **Experiments.** We evaluate EnsembleCert on ensembles with finite-width linear networks as base  
1644 classifiers by applying the gradient-based certificate to each base classifier. As described in the pre-  
1645 vious section, this certificate can be incorporated into EnsembleCert. Briefly, for each sample we  
1646 compute the minimum number of label flips required to change the prediction of base classifier  $i$  to  
1647 *some* class by applying the gradient-based certificate over increasing budgets until robustness fails.  
1648 We then use this value as  $\rho_i^c$  for every class  $c$ . Because this incremental application of the gradient-  
1649 based method is computationally demanding, our experiments on finite-width models are limited to  
1650 CIFAR-10 and a small number of partitions. Nevertheless, as shown in Fig. 8, incorporating white-  
1651 box information through EnsembleCert substantially improves certified accuracy. This demonstrates  
1652 that EnsembleCert extends naturally to ensembles built from finite-width neural networks. More-  
1653 over, the integration procedure highlights a broader utility: any certificate that determines whether a  
1654 model remains robust up to a given number of label flips can be adapted to certify the base classifiers  
1655 within EnsembleCert.

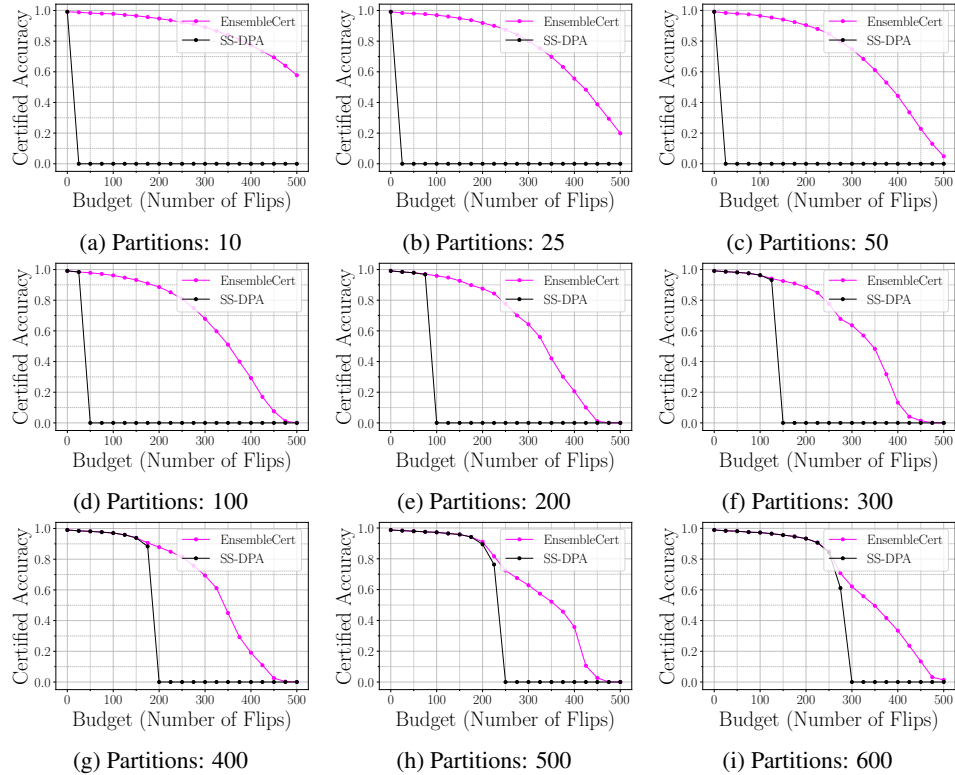


1667 Figure 8: EnsembleCert evaluated on ensembles with finite-width network as base classifiers. The  
1668 base classifiers are certified by applying the gradient-based bounding technique by Sosnin et al.  
1669 (2024). Evidently, EnsembleCert significantly outperforms SS-DPA, the black-box approach applied  
1670 to the ensemble.

1674 C.5 ROBUSTNESS TRENDS ACROSS  $\lambda$  FOR ENSEMBLECERT WITH KERNEL REGRESSION  
1675

1676 We study the effect of the  $\mathcal{L}_2$  regularization parameter  $\lambda$  on certified robustness. For low  $\lambda$ , the  
1677 MCR increases with the number of partitions across all datasets. In contrast, for high  $\lambda$ , the **certified**  
1678 **robustness appears to be negatively affected by increasing the number of partitions**. The  
1679 contrasting behavior potentially arises due to the varying degree of robustness that the choice of  $\lambda$   
1680 imparts the base classifier. Low  $\lambda$  makes kernel regression unstable, causing base classifiers to be  
1681 easily influenced by a few label flips, even with large partitions. In this regime, the ensemble is  
1682 closer to the black-box assumption - that a single label flip can change a base classifier's prediction  
1683 - even when the number of partitions is small, resulting in white-box certificates that aren't much  
1684 tighter than the black-box ones. In contrast, using a high degree of regularization exhibits a substan-  
1685 tial improvement in the certified accuracy on white-box infusion. Fig. 10 shows how the robustness  
1686 trend changes with varying  $\lambda$  for CIFAR-10. While at  $\lambda = 0.01$ , the median certified robustness  
1687 scales almost linearly with the number of partitions, the trend completely changes by the time we  
1688 reach  $\lambda = 100$ . Empirical analysis suggests that the nature of the trend changes somewhere between  
1689  $\lambda = 1$  and  $\lambda = 5$ . Interestingly, the change in trend also points towards the possibility that for  
1690 some value between  $\lambda = 1$  and  $\lambda = 5$ , the median certified robustness could exhibit invariance to  
1691 the number of partitions, a phenomenon we observed with kernel SVMs. Similar behavior is seen  
1692 for experiments on MNIST as well (Fig. 9). As we mentioned in Sec. 4, the threshold  $\lambda$ , where the  
1693 behavior changes is data dependent.

1701 Figure 9: Robustness trends across different  $\lambda$  values on MNIST using kernel regression.1722 Figure 10: Robustness trends across different  $\lambda$  values on CIFAR-10 using kernel regression.

1728  
1729 C.6 MNIST 1-vs-71730  
1731 **Kernel Regression.** We present results for evaluation using kernel regression with NTK and the  $\ell_2$   
1732 regularization parameter  $\lambda = 0.1$  in Fig. 11.1758 Figure 11: MNIST binary kernel regression with  $\lambda = 0.1$  results for different number of partitions.  
17591760 **Kernel SVM**  
17611762 We present results for evaluation using kernel SVM with NTK and a sufficiently small  $C$  in Fig. 12.  
1763

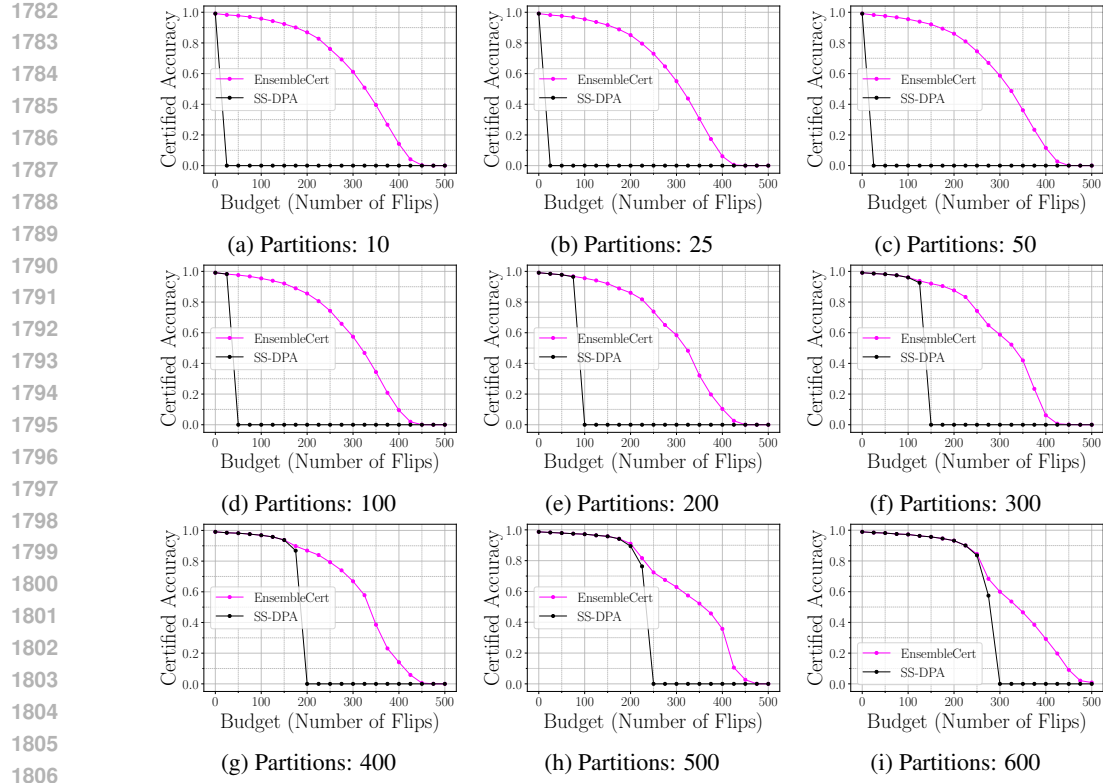


Figure 12: MNIST binary kernel SVM results for different number of partitions.

1810  
1811  
1812  
1813  
1814  
1815  
1816  
1817  
1818  
1819  
1820  
1821  
1822  
1823  
1824  
1825  
1826  
1827  
1828  
1829  
1830  
1831  
1832  
1833  
1834  
1835

**MCR results** Consistent with the results on MNIST and CIFAR10, Fig. 13 demonstrates the invariance of median certified robustness to the number of partitions, for both kernel Reg and kernel SVM

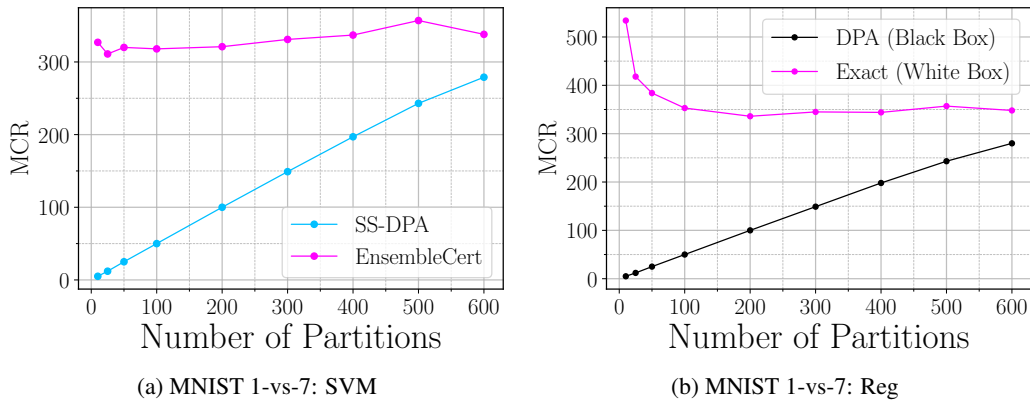
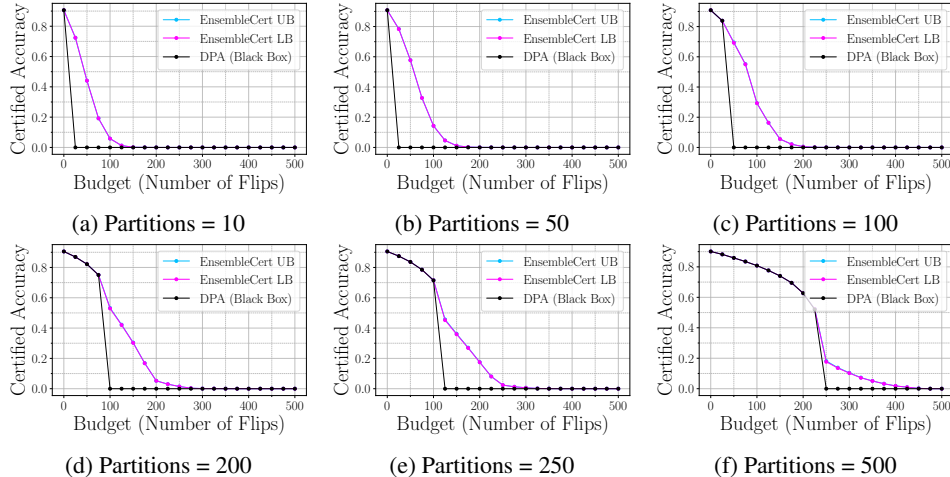
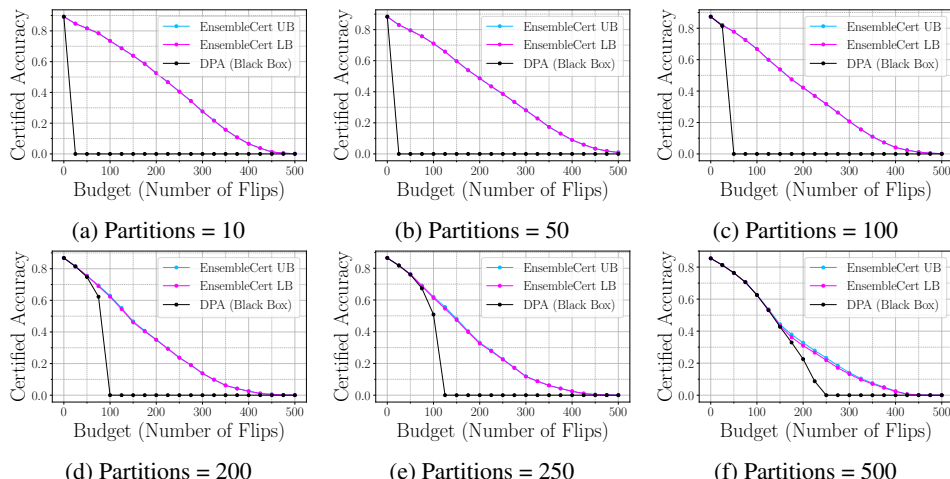


Figure 13: Invariance to number of partitions

1836 **C.7 CIFAR-10**  
18371838 **Kernel Regression**  
1839

1840 For low values of  $\lambda$ , the base classifier by itself is not robust and is closer to the worst-case black  
1841 box assumption described in App. A.1. Consequently, we do not see a significant improvement  
1842 on utilizing white-box knowledge of the base classifiers. This is illustrated in Fig. 14, where we  
1843 evaluate EnsembleCert using kernel regression as base classifier and a low regularization parameter  
1844  $\lambda = 0.01$ . In contrast, using a high degree of regularization changes the trend as mentioned in the  
1845 experiments section. In this case, we see a substantial improvement in the certified accuracy on  
1846 white-box infusion. The results on using a high lambda can be seen in Fig. 15.

1863 **Figure 14: CIFAR-10 kernel regression results for different numbers of partitions ( $\lambda = 0.01$ ).**1881 **Figure 15: CIFAR-10 kernel regression with high regularization ( $\lambda = 10$ ).**  
1882  
1883  
1884  
1885  
1886  
1887  
1888  
1889

1890

**Kernel SVM**

1891

1892 Substantial improvement can be observed in certified accuracy on white-box infusion, as seen in  
 1893 Fig. 16.

1894

1895

1896

1897

1898

1899

1900

1901

1902

1903

1904

1905

1906

1907

1908

1909

1910

1911

1912

1913

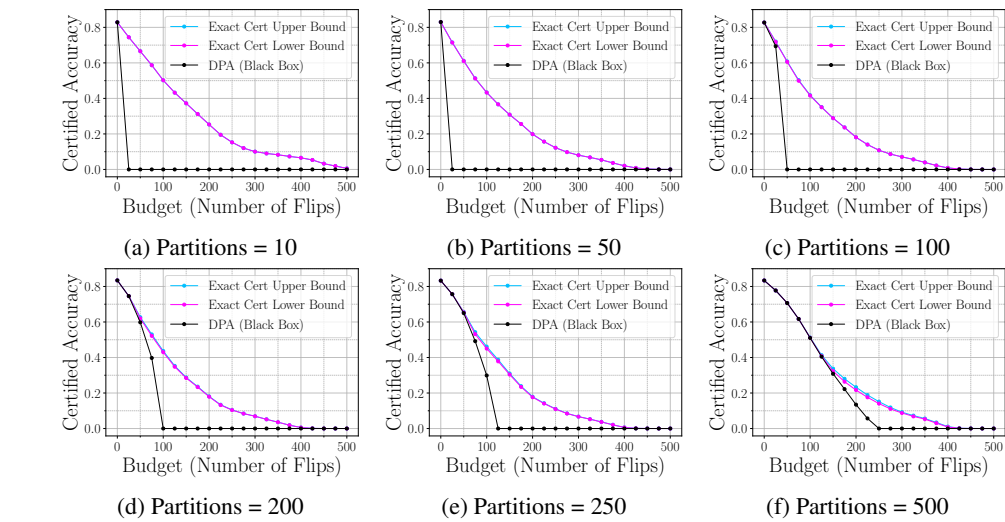


Figure 16: CIFAR-10 kernel SVM results for different numbers of partitions.

1914

**Smoothed linear classifier**

1915

1916 Similar to kernel regression and kernel SVM, substantial improvement is observed in certified accuracy on white-box infusion, as shown in Fig. 17.  
 1917

1918

1919

1920

1921

1922

1923

1924

1925

1926

1927

1928

1929

1930

1931

1932

1933

1934

1935

1936

1937

1938

1939

1940

1941

1942

1943

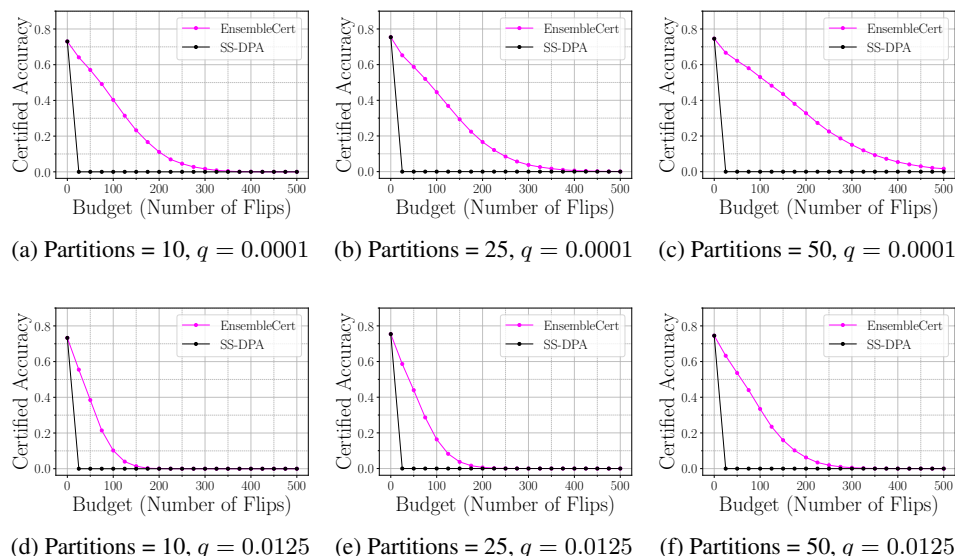


Figure 17: CIFAR-10 Smoothed linear regression as base-classifier

1944  
1945

## C.8 MNIST

1946

## Kernel Regression

1947

We analyze the low and high regularization parameter  $\lambda$  on MNIST. Similar to CIFAR-10, we observe that for low values of  $\lambda$ , the base classifier by itself is not robust and is closer to the worst-case black box assumption described in App. A.1. Consequently, we do not see a significant improvement in utilizing white-box knowledge of the base classifiers. This is illustrated in Fig. 18 using low  $\lambda = 0.0001$ . In contrast, using a high degree of regularization changes the trend. In this case, we see a substantial improvement in the certified accuracy on white-box infusion. The results on using a high lambda can be seen using high  $\lambda = 0.1$  in Fig. 19.

1948

1949

1950

1951

1952

1953

1954

1955

1956

1957

1958

1959

1960

1961

1962

1963

1964

1965

1966

1967

1968

1969

1970

1971

1972

1973

1974

1975

1976

1977

1978

1979

1980

1981

## Kernel Regression

We analyze the low and high regularization parameter  $\lambda$  on MNIST. Similar to CIFAR-10, we observe that for low values of  $\lambda$ , the base classifier by itself is not robust and is closer to the worst-case black box assumption described in App. A.1. Consequently, we do not see a significant improvement in utilizing white-box knowledge of the base classifiers. This is illustrated in Fig. 18 using low  $\lambda = 0.0001$ . In contrast, using a high degree of regularization changes the trend. In this case, we see a substantial improvement in the certified accuracy on white-box infusion. The results on using a high lambda can be seen using high  $\lambda = 0.1$  in Fig. 19.

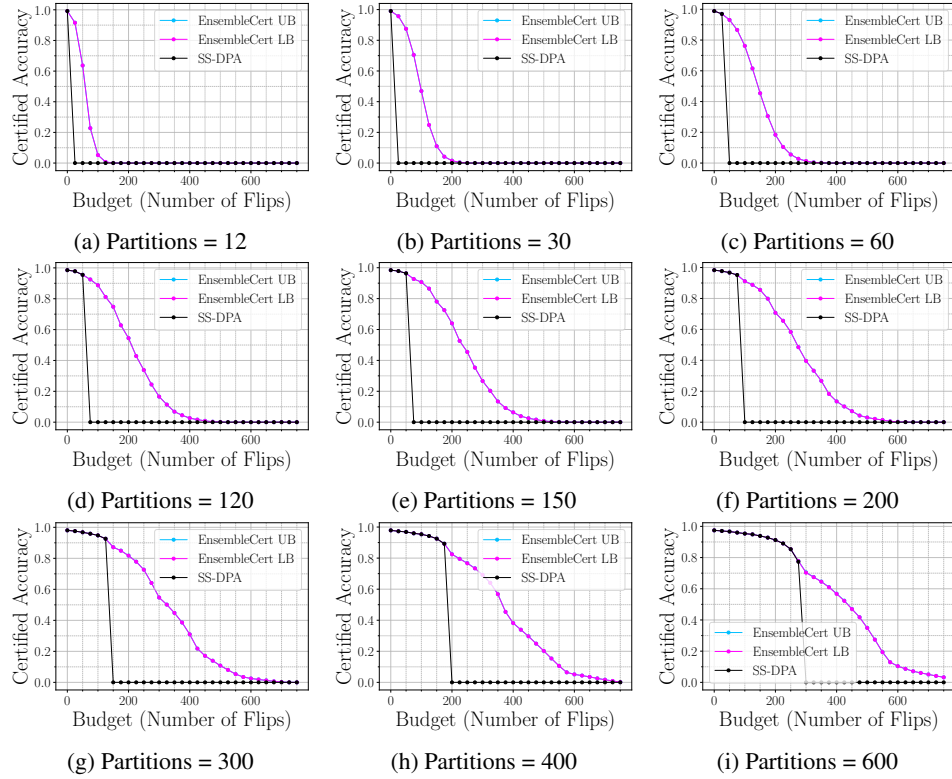


Figure 18: MNIST multi-class kernel regression results for different numbers of partitions ( $\lambda = 0.0001$ ).

1982

1983

1984

1985

1986

1987

1988

1989

1990

1991

1992

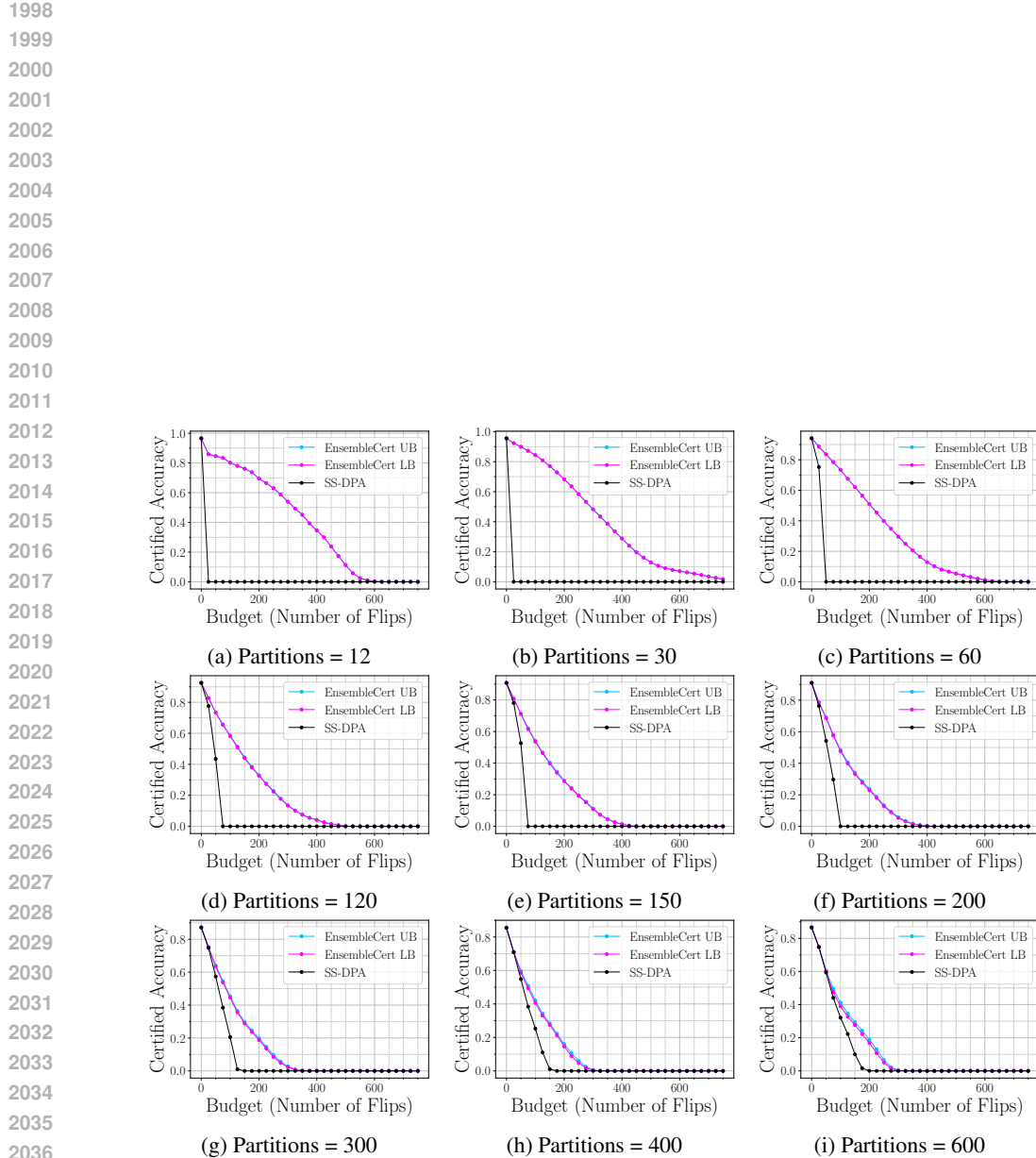
1993

1994

1995

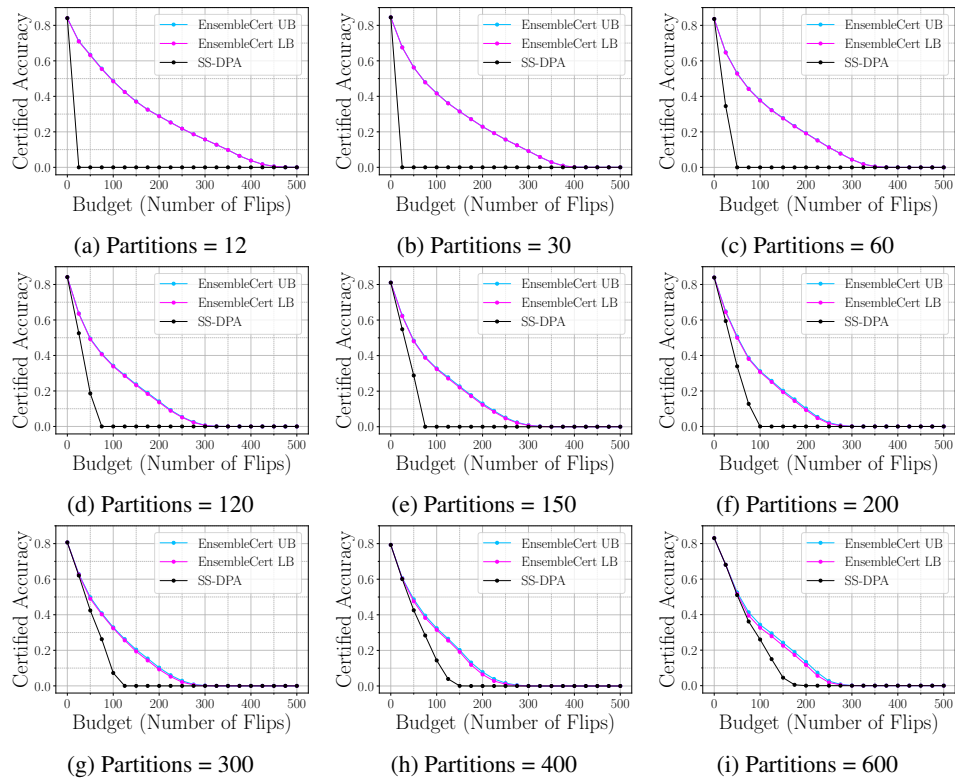
1996

1997

Figure 19: MNIST multi-class kernel regression results for different numbers of partitions ( $\lambda = 0.1$ ).

**2052 Kernel SVM**

2053  
 2054 Results showing substantial improvement in the certified accuracy on white-box infusion for kernel  
 2055 SVM are observed in Fig. 20.



2056  
 2057  
 2058  
 2059  
 2060  
 2061  
 2062  
 2063  
 2064  
 2065  
 2066  
 2067  
 2068  
 2069  
 2070  
 2071  
 2072  
 2073  
 2074  
 2075  
 2076  
 2077  
 2078  
 2079  
 2080  
 2081  
 2082  
 2083  
 2084  
 2085  
 2086  
 2087  
 2088  
 2089  
 2090  
 2091  
 2092  
 2093  
 2094  
 2095  
 2096  
 2097  
 2098  
 2099  
 2100  
 2101  
 2102  
 2103  
 2104  
 2105  
 Figure 20: MNIST multi-class kernel SVM results for different numbers of partitions.